Università degli Studi di Cagliari

PHD COURSE

IN MOLECULAR AND TRANSLATIONAL MEDICINE

CYCLE XXX

THESIS TITLE

ANALYSIS AND EVALUATION OF CLINICAL AND PREDICTIVE BIOMARKERS OF RESPONSE TO IMMUNOTHERAPY IN THE ONCOLOGICAL FIELD

Scientific Disciplinary Sector

……

Presented by: Laura Orgiano, MD

Course Coordinator Amedeo Columbano, PROF

Tutor Clelia Madeddu, MD, PROF

Final Examination Academic Year 2016 – 2017

Thesis discussed in the February examination session 2018

Index

Immune system and cancer
Cancer Immunosurveillance
Immunoediting
Immune Checkpoints
CTLA-4 (Cytotoxic T-Lymphocyte Antigen-4)
PD-1 (Programmed cell death protein-1)
Co-stimulatory receptors
Mirobiote and Immune System
Intestinal Microbiote
Microbial composition
Molecular interactions between bacteria, epithelium and mucosal immune system

Patients and Methods
CARAMEL Study Design
CREAM Study Design
COFFEE Study Design
Parameters evaluated
Clinical Parameters
Statistical analysis

Extraction of genomic DNA from stool

CARAMEL STUDY - RESULTS
Characteristics of patients
Survival analysis
Prognostic value of clinical and laboratory parameters in terms of OS and PFS
Clinical parameters
Laboratory parameters
Correlation analysis between clinical and laboratory parameters and OS and PFS data

CREAM STUDY – RESULTS
COFFEE STUDY – RESULTS

Bibliography

Immune system and cancer

The immune system is the guardian of the integrity of our body: it protects us from infections due to environmental pathogens but also from other types of invasions strangers, such as transplants and neoplasms. Immunology and oncology have a long time relationship and the two fields have intersected several times throughout the last half century.
The correlation between immune system and tumor pathology is already known since the last century: in 1890 William Cooley had observed that some patients suffering from solid tumors assessed a spontaneous remission after contracting an acute infection (Cooley, 1890). Cooley himself developed a bacterial concentrate of killed colonies of Streptococcus pyogenes and Serratia marcescens (Cooley's toxin) which inoculated directly into the tumor site, causing fever in the host and, in some cases, also therapeutic benefits, eventhough his work was soon shadowed by the advent of X - rays and, later, by chemotherapy.
During the mid-twentieth century, Richmond Prehn and Joan Main showed how solid tumors induced by chemical carcinogens, once transplanted into the mouse, can stimulate an immune response tumor-specific capable of rejecting the tumor itself (Prehn and Main, 1957). A few years later, based on the observation of mouse models, Lewis Thomas e McFarlane Burnet proposed the theory of Cancer Immunosurveillance, hypothesizing that the immune system could be able to destroy cancer cells (Burnet, 1970; Thomas, 1982).
In 1991, the antigenic structure and the coding gene sequences were identified and it was demonstrated how they were recognized by T cells (Van der Bruggen, 1991): this discovery generated a wave of optimism about vaccines and the immunomodulatory approach in therapeutic field against cancer. Indeed, in 1995 and 1998 two inflammatory cytokines, INF-α and IL-2, were approved for the treatment of cutaneous melanoma in the adjuvant and metastatic setting, respectively. The immunotherapy approaches developed in those years had limited benefits in terms of overall survival, mostly restricted to a limited number of patients, but the international scientific community did not leave this research field [**[1]**].

Cancer Immunosurveillance

From his first enunciation by Burnet in 1970, the theory of Immunoassay was then developed at the preclinical and clinical levels by several researchers. Immunoassay provides that the same immune components which can eliminate any other pathogens, in an immune-responsible organism, can notice the presence of cancer cells and destroy them as well. This hypothesis is indirectly demonstrated by the incidence of different types of cancer in patients with HIV/AIDS and in organ transplant patients, significantly higher
If compared with that of healthy population. Therefore, the chronic immunodepression typical of these patients, is responsible for the increased risk of new cases tumor [**[2]**].
Our immune system is a complex and well balanced system consisting mainly of two types of response: innate immunity (fast, non-specific antigen) and adaptive immunity (it activates later, it is antigen-specific, it mediates the immune memory). Eventhough the cellular components of both systems are able to recognize and destroy tumor cells when activated, the mechanism of immunosorveillance against tumor cells is based mostly on the action of T lymphocytes. The importance of this Cellular component has been proven in mouse models: timectomy or the removal of T lymphocytes causes uncontrolled tumor growth [**[3,4]**]. In addition, in human models it has been seen as some hystologic types of neoplasms, such as lung and colorectal cancer, are often infiltrated by T lymphocytes, in particular CD8 +, and that the grade of the infiltrate is

associated with a favorable prognosis: these evidences have led to the development of a study for validating an algorithm, the Immunoscore, which evaluates the prognostic impact of the presence of TIL (tumor-infiltrating lymphocyte) and it aspires to modify the current TNM classification, based at the moment only on the tumor burden (T), on the presence of regional lymph node tumor cells (N) and distant metastasis (M) [5,6].

We know that the tumor is characterized by a huge variable number of gene alterations and the loss of normal adjustment processes. These events lead to the expression of neo-antigens which lead to the presentation of peptides bound to the class I molecules of the MCH system on the surface of cancer cells: from several studies from Boon et al., we know now that these tumor-specific peptide complexes / MCHIs are recognized by T CD8 + lymphocytes, thanks to the T cell receptor (TCR) (Boon, 1994). Following recognition of specific tumor antigen, T CD8 + (cytotoxic) lymphocyte releases cytotoxic granules that induce an osmotic shock and so the cell death. Indeed, CD4 + (helper) lymphocytes release other cytokines, such as IL-2, able to promote proliferation and lymphocytic activation to support and amplify the immune response.

In any case, even when the T lymphocyte response is activated, in order to have an antitumoral immune response it is necessary also the presence of other immune cellular components, so they all together can activate a series of waterfall and crossed events, better defined as the Cancer-Immunity Cycle (Figure 1).

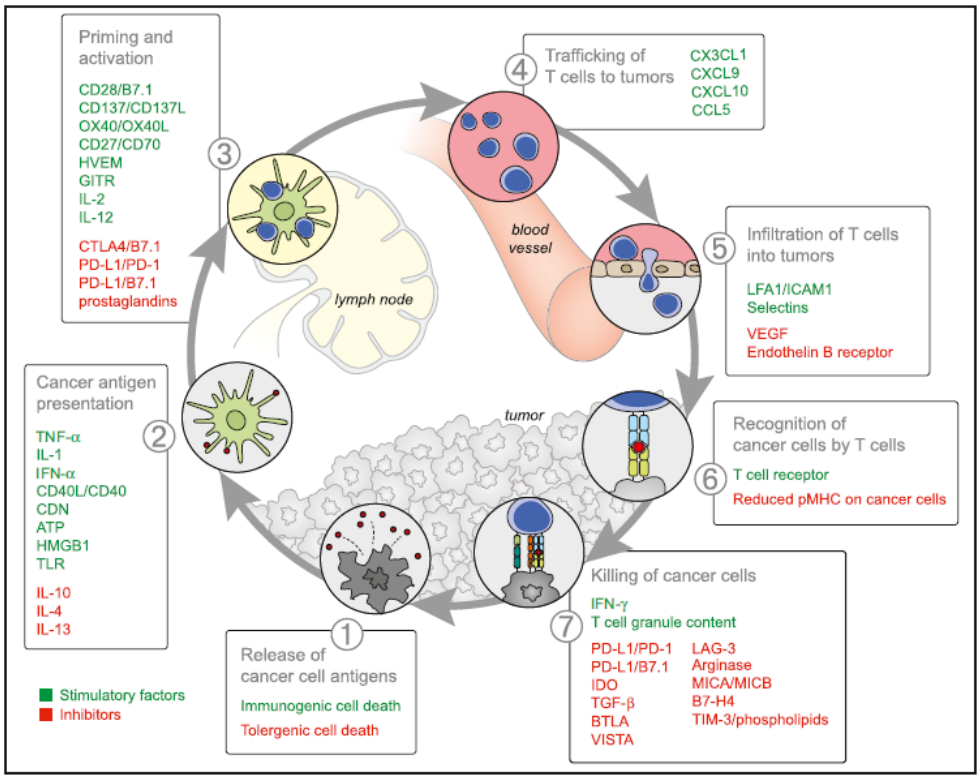

Figure 1. Cancer Immunity Cycle. Chen DS, Mellman I. oncology meets immunology: the cancer immunity cycle. Immunity 2013; 39(1): 1-10.

As a first step, Natural Killer (NK) cells destroys some other cells of the same tissue as a result of their uncontrolled growth: this causes the release of cellular debris, that behave like tumor antigens and they are captured and internalized by dendritic cells (DCs), normally present at the tissue level as well. To ensure that these events can then produce a T cell-mediated antitumoral response, they should be further actived by the release of other immunogenic signals, such as

proinflammatory cytokines and other factors released bybosmotic destruction of the tumor cell or intestinal microbiotomy.
Subsequently, dendritic cells process the tumor antigen and they present it on their surface once in connection with class I and II MCH molecules (step 2). The antigen presentation allows DCs to activate antigen-specific T lymphocytes (CD8 + cytotoxic and CD4 + helper) and to induce their clonal expansion (step 3). The nature of the immune response is basic in this stage, because of the critical equilibrium between T effectors lymphocytes and T regulatory lymphocytes. Finally, T effectors lymphocytes move to the tumor bed (step 4) and they infiltrate it (step 5). T lymphocytes at this point are able to recognize the tumor cells, thanks to the interaction between their TCR and the MCH class I antigens on the surface of the tumor cells (step 6), leading to their death (step 7). This process results in the release of additional tumor-associated antigen (step 1, again) leading to the self-feeding of the loop [3,7].

Immunoediting

In cancer patients, the Cancer-Immunity cycle does not work optimally. The tumor antigens cannot be detected so easily: DCs and T lymphocytes can treat the tumor antigen as part of the self instead of non self, resulting in a displacement between effector lymphocytes and regulator lymphocytes; so lymphocytes may not reach or infiltrate properly the tumor bed or, mostly important, some factors of the tumor microenvironment can suppress the effector cells produced[7]. Therefore, in the last fifteen years, the concept of immunotherapy has been further refined and extended, leading to concept of Cancer Immunoediting, in order to describe the many interactions between immune system and solid tumors.
This dynamic process consists mainly of three phases: elimination, equilibrium and escape.
Elimination is the first phase of immunoediting: the innate immunity and the one adaptive co-work to identify and destroy early stage neoplasms before they become clinically visible. At this stage, the balance is on the side of antitumoral immunity, due to an increase in the expression of tumor antigens, class I MCH, Fas and TRAIL receptors on tumor cells and perforins, granulocyte enzymes, INF- α / β / γ, IL-1, IL-12, TNF-α in the tumor microenvironment (Figure 2a).

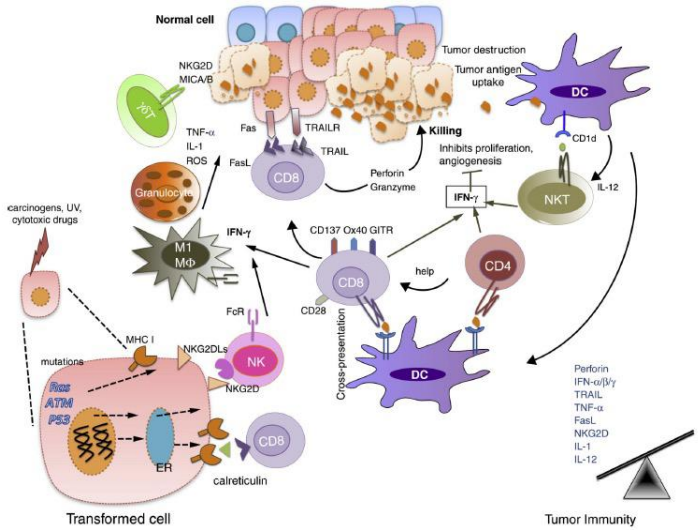

Figure 2a. Elimination

Subsequently, in the equilibrium phase, the immune system and tumor growth are
in a kind of functional quiescence: some cancer cells develop genetic and epigenetic changes due to continued immune pressure (loss of surface antigens or deficiency of antigen presentation) and the expression of PDL1. So, in tumor micro-environment there is a perfect balance between antitumor cytokines (IL-12, INF-γ) and pro-tumoral ones (IL-10, IL-23) (Figure 2b).

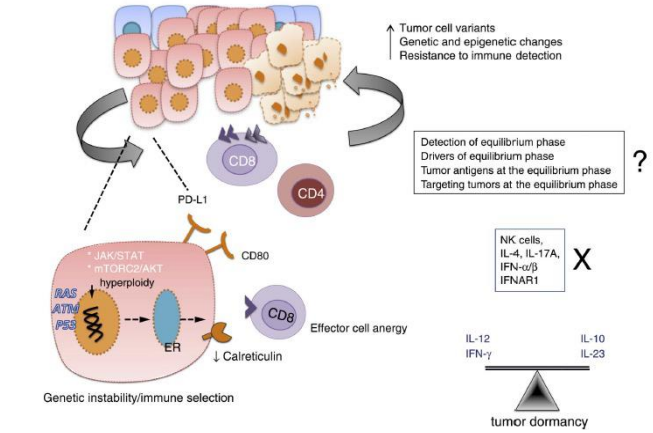

Figure 2b. Equilibrium.

Finally, in the escape phase, the tumor progressively avoids the immune control and survives in the host (Figure 2c).

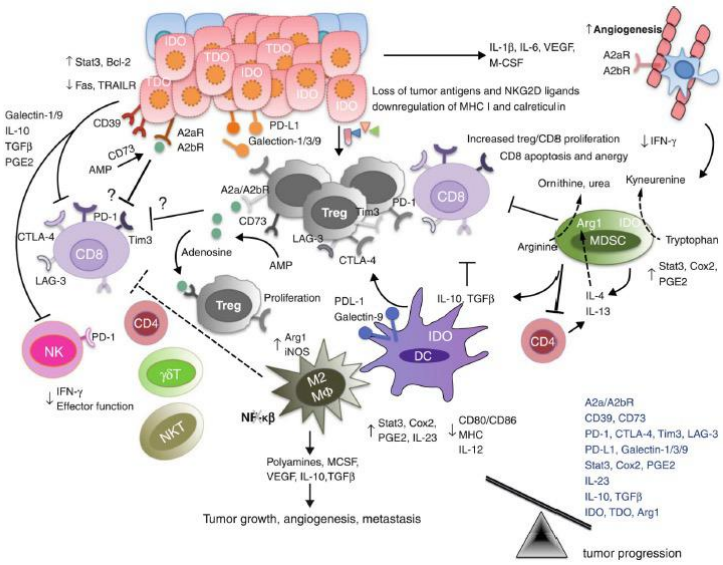

Figure 2c. Escape.
Figure 2a,b,c. Immunoediting. *Mittal D, Gubin MM, Schreiber RD, et al. New insights into cancer immunoediting and its three component phases. Curr Opin Immunol 2014; 27:16-25.*

From this point of view, the type of response the immune system puts into action is different if comparing a bacterial or viral infection or tumor pathology. In the presence of acute infection, specific T lymphocytes are generally able to eliminate the pathogen and therefore the antigenic stimulus. When this happens, the cells of the Immune response are controlled by negative feedback mechanisms and the immune response shuts off. A small proportion of specific lymphocytes however remains silent, ready to trigger the response in case the pathogen should appear again (immunological memory). In the case of tumors, where the antigen quite rarely is eliminated, there is a chronic immune stimulation.

Chronic immune stimulation is determined by the continuous release of the antigen, and it leads to the activation of negative feedback and a progressive mechanisms of depletion of cytotoxic capacity of T lymphocytes (exhaustion). At the same time, immunosuppressive cells, such as

regulatory T cells and suppressive myeloid cells, are linked at the tumor site by multiple mechanisms, and they contribute to keep the immune response silent. The tumor itself activates immunosuppressive mechanisms and strategies to reduce immunomedial recognition. With the progression of disease, the tumor cell acquires the ability to express molecules that can inhibit the immune response (PDL-1, TGFbeta IL-10, iNOS), or it can reduce the expression of the complex HLA/antigen which initially made it identifiable by T lymphocytes: these strategies, along with others, give the tumor cell the ability to undo the attempts of our defenses to control tumoral growth.

Although in the subclinical phases of the disease, the immune response can be try in some way to contain tumoral growth or even eliminate the tumor, it is pretty sure that the tumor is in the escape phase when the patient comes to our attention [***3, 8***].

Immune Checkpoints

We have just seen that during the escape process the tumor can develop a several number of strategies through which escape control by the immune system, primarily by increasing the immunosuppressive cell population, with massive infiltrate of regulatory T cells and suppressive myeloid cells, and through the production of soluble immunosuppressive agents. The tumor cells and the nearby stromal cells produce anti-inflammatory cytokines such as TGF-β, IL-10 and enzymes; the micro environment also determines the expression of molecules that act as immunological checkpoints: CTLA-4 and PDL-1 are strongly expressed on T cells and cancer cells, respectively.

In physiological conditions, the main role of immune checkpoints is to protect from the damage that may occur when the immune system responds to pathogens and to maintain tolerance to self antigens, avoiding autoimmunity mechanisms. This step is achieved by decreasing the number of T effector cells and their functions.

The scientific data collected in recent years show that the main mechanism used by tumors to elude the immune system is through the use of immunological checkpoints. This observation has stimulated the development of several drugs able to modulate these targets or other costimulatory receptors [**9,10**].

CTLA-4 (Cytotoxic T-Lymphocyte Antigen-4)

We have seen how activation (better known as priming) of naïve T cells should be triggered by APCs (antigen-presenting cells), essentially represented by dendritic cells. After the internalization and processing of antigen, dendritic cells present the antigenic peptide bound to MHC class I and II molecules. Two "signals" are required because the APC is recognized as a non self and the immune response is triggered.

"Signal 1" is determined by the recognition of the peptide/MHCI complex by the TCR of the T lymphocyte, whilst "signal 2" occurs in response to the binding of the CD80 (or B7) and CD86, both present on the surface of the APC, with the CD28 receptor, constitutively expressed on the surface of T lymphocytes. The "signal 2" is, therefore, a co-stimulation signal needed for optimal activation of T lymphocyte.

This interaction determines the secretion of IL-2, which induces proliferation and differentiation of effector T cells. Although cancer cells themselves can behaving as APCs, they are not able to

directly activate T naive lymphocytes: they usually do not have any expression of CD80 and CD86 on their surface and therefore can not provide the co-stimulatory signal.
"Signal 1" alone is not enough to trigger T cell response and can cause an anenergy.
Under normal conditions, once activated T lymphocytes have exhausted their task, they undergo to an inhibition process, that limits the proliferative response of activated T cells to maintain peripheral tolerance and to prevent tissue damage, due to an excessive activation. This inhibition occurs thanks to the binding between CD80 and CD86, both present on the APCs surface, with the CTLA-4 expressed on the cell surface of the activated T lymphocytes.
CTLA-4 is a CD28 homologue, a member of the superfamily of immunoglobulins (Brunet, 1987). It is not found on the surface of quiescent T lymphocytes: the expression of CTLA-4 is induced by the activation of T cell lymphocytes, so CTLA-4 moves from the intracellular to the extracellular compartment, where it remains up-regulated for two-three days after activation of the lymphocyte.
CTLA-4 binds CD80 and CD86 with an affinity approximately a hundred times greater than the one to the CD28 receptor; this competitive link with CD28 "shuts off" the activation of T lymphocytes: this turns the activated lymphocyte population into a small pool of memory cells. CTLA-4, therefore, represents an important inhibitory signal that controls the duration and intensity of the immune response.
There is ample evidence that supports the critical role of CTLA-4 in the normal immune function. For example, CTLA-4 genetic deficiency males develop lymphoproliferative diseases, characterized by uncontrolled proliferation of lymphocytic cells accompanied by tissue infiltration, multi-organ dysfunction syndrome and early death. In humans CTLA-4 polymorphisms are related to a wide range of autoimmune disorders such as thyroid disorders, Addison's disease, diabetes mellitus type 1, rheumatoid arthritis [**11**].
Likewise, patients suffering from melanoma with polymorphism associated with a reduced expression of CTLA-4 showed a more pronounced response to treatment with CTLA-4 inhibitor, with an increase of immune-correlated side effects and less chance of recurrence of disease [**12**]. Finally, it was seen that in patients with allogeneic allograft melanoma, the expression of CTLA-4 post-vaccination was inversely related to survival [**13**].

PD-1 (Programmed cell death protein-1)
Whilst CTLA-4 primarily regulates the activation of T cells in lymphoid tissues, the main role of PD-1 is to limit the activity of T lymphocytes in peripheral tissues during a cell-mediated or inflammatory immune response.
PD-1 expression is induced in activated T cells: when PD-1 is bound by one of its ligands, it recovers SHP2 phosphatase and it causes a decrease in signal transduction of TCR on the membrane surface, modifying the duration of the contact between activated T cell and APCs or tumor target cell.
Similarly to CTLA-4, PD-1 is extensively expressed on the surface of regulatory T cells, to promote their proliferation once bounded with ligand.
Since many tumors are massively infiltrated by regulatory T cells, the blockade of PD-1 pathway can induce the anti-tumor immune response by decreasing the number and/or immunosuppressive activity of intratumoral regulatory T cells.
The two PD-1 ligands are PDL-1 (also known as B7-H1 or CD274) and PDL-2 (also known as B7-DC or CD273): the interaction with these ligands limits the inflammation and inhibits the activity of T lymphocytes in the tissue and in the tumor microenvironment. Recently, an unexpected interaction has also been observed between PDL-1 and CD80 (Butte, 2007), but the relevance of this interaction in tumor immune suppression has not yet been exactly determined.

PD-1 is also expressed by B cells and NK cells, limiting in this last case their lithic activity: the expression also in these non-T cell types could be used by the pharmacological block of PD-1 to induce the activity of NK tumor cells and to promote the production of antibodies by B cells.
PD-1 is expressed in infiltrating lymphocytes (TIL, tumor-infiltrating lymphocytes) in several histological tumor types: at this level it induces the apoptosis of the T lymphocytes and it induces the differentiation of CD4 + lymphocytes in regulatory T cells. PDL-1 is the mostly expressed ligand and, with PDL-2, they are commonly up-regulated on the cell surface. It has been seen in mouse models that a higher induced expression of PDL-1 inhibits the antitumoral T-mediated response . PDL-1 is constitutively expressed on macrophages, PDL-2 is expressed on macrophages and dendritic cells, although is less well known its impact on control of the immune response.
In the field of renal cancer, the expression of PDL-1 in the tumor and in TIL predictes a worse prognosis than PDL-1 negative tumors; after this discovery, they extended the analysis to other histological tumor types: further evidence suggested that PDL-1 status may be related to bad prognosis, better prognosis, or no correlation with prognosis.
Probably many factors influence the wide range of clinical outcomes reported by these patients (immunohistochemical determination technique of PDL-1 Expression, Primitive Lesion vs. Metastatic lesion, histological type, stage of disease, treatment lines previously performed).
Considering the heterogeneity of expression of PD-1 ligands and their potential relevant role as biomarkers in the pharmacological block of PD-1 pathway, different PDL-1 Expression Control Mechanisms have been studied: two main mechanisms have been involved, the innate immune resistance and the adaptive immunoreactivity.
For some tumor types, such as glioblastoma, PDL-1 is constitutively expressed on the cell surface (innate immune resilience).
The other mechanism, the adaptive immunoreactivity, is based on the physiological induction of PD-1 ligand expression that normally protects tissues from excessive inflammatory reaction: expression of PDL-1 occurs in this case in response to secretion into the microenvironment
tumor of interferons, in particular of IFN-γ. Gajewski et al. have shown that melanoma can be divided into approximately two categories, inflammatory and non-inflammatory, based on pro-inflammatory gene expression, including metabolic pathways leading to IFN-γ secretion, and it has been demonstrated a correlation between PDL-1 expression on tumor cell surface and the expression of IFN-γ in the intramural lymphocyte infiltrate. These observations suggest the presence of negative feedback where IFN-γ induces expression of PDL-1 which suppresses the activity of T PD1 + lymphocytic cells (Figure 3) [**14**].

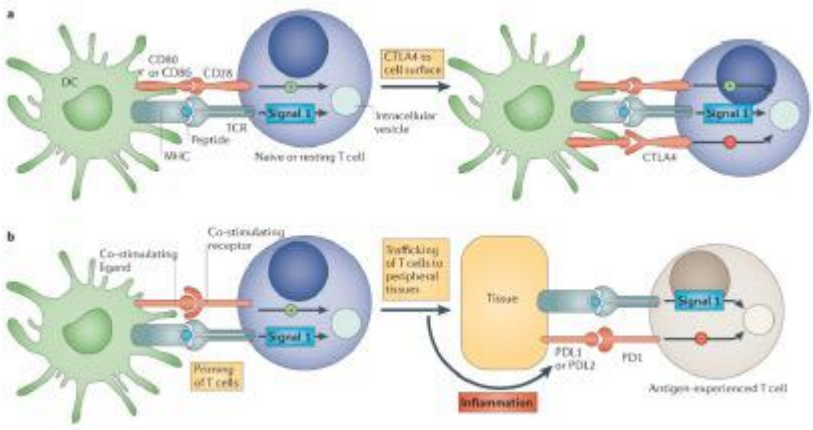

Figure 3. Immune checkpoint blockade CTLA4 e PD1. Pardoll DM. The blockade of immune checkpoints in cancer immunotherapy. Nat Rev Cancer 2012; 12(4):252–264.

Co-stimulatory receptors

In addition to the CTLA-4 and PD-1 pathway studied, further studies are being carried out to identify additional therapeutic targets in co-stimulatory receptors: for example, OX40 expressed in CD4 + and CD8 + cells; CD137, member of the TNF receptor superfamily; ICOS, a specific T cell stimulation molecule.

Mirobiote and Immune System

Intestinal Microbiote

The human gastrointestinal system represents one of the ecosystems with the highest density of microbial population present in nature. The size of the human intestinal microbiote, with a number of 1013-1014 microorganisms and a biomass weight of about 1 kg, far exceed those of other microbial communities in the human body, and they are about ten times higher than the total somatic and germinal cell ([15]). The microbiote is a "metabolic organ" able to influence and regulate many systemic functions, it contributes to keep health, and we now it plays a key role in the pathogenesis of many gastrointestinal (irritable colon, chronic inflammatory diseases, diverticolitis, colon cancer) and systemic diseases (allergies , obesity, type 2 diabetes, atherosclerosis) ([16]). The intestinal microbiote begins its development already in the uterus ([17]) and during the early stages of neonatal life the bowel is further colonized by maternal and environmental microorganisms (Figure 4).

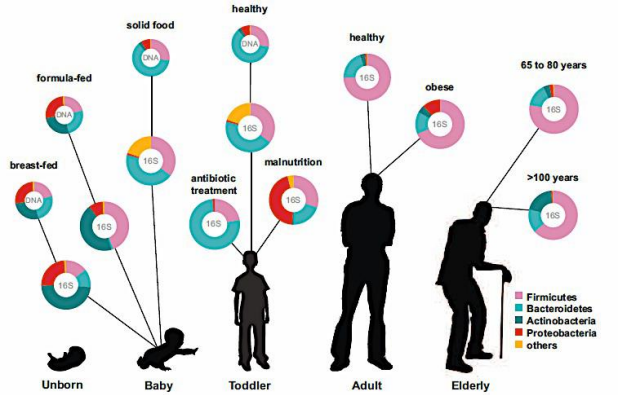

Figure 4. Changes of human intestinal microbiology according to age

Recent studies have shown that human intestinal microbiology varies according to age ([18]). At about 4-5 years of age, the intestinal microbiote is dominated by two phyla, Firmicutes and Bacteroidetes; once the microbiote is formed, its composition remains almost constant during adulthood. In the older age, some changes are noticed again: there is an increase in levels of Lactobacilli, Coliforms, Clostridium, Enterococci and a decrease in Bifidobacteria levels ([18]).

The adult intestinal microbiota remains relatively stable over time, with the exception of possible variations due to several environmental factors, eating habits or pathogenesis ([19, 15, 20]). It seems that diet greatly affects the composition of the intestinal microflora, although the various studies conducted have not yet been able to quantify this correlation due to the wide variability observed by one person per person ([21]). The influence of diet on the composition of microbial flora has been evident since the first months of life, where the major differences are found in the composition of bifidobacteria. A number of studies have shown how the food regime can significantly affect the intestinal ecosystem of the adult subject. A study by Hayashi H et al. ([22]), for example, showed marked differences in faecal microbial of vegetarian subjects compared to omnivorous subjects: the microbiota of vegetarian subjects examined showed a percentage of Bacteroidetes equal to about 6% whole microbiota, against 25% of subjects undergoing a normal diet, while the Faecalibacterium prausnitzii species was not detected while being one of the major components of the microbiota. A hyperlipidic diet causes considerable modifications in the composition of the microbiota, the percentage of Firmicutes present increases considerably at the expense of phylum Bacteroidetes.

Microbial composition

The human intestinal microbiote is represented by a set of bacteria, archeobacteria, eukaryotes and viruses living in the digestive channel. In healthy subjects, the gastrointestinal tract hosts between 500 and 1000 different species of bacteria which maintain in physiological conditions a symbiotic relationship with the host. The number of bacterial cells is ten times greater than the number of human eukaryotic cells ([23]). From recent several molecular biology studies based on the sequencing of the region encoding the 16S bacterial ribosome, it has been found that most faecal bacteria belongs to two of the major phylogenetic strains: Bacteroidetes and Firmicutes. However,

the greatest number of discoveries regarding microflora are often related to only faecal specimens: there are little studies on ascending colon microflora; Similarly, we have little information about the microflora sticking to the walls of the colon itself. Most intestinal microbial communities belong to the kingdom of Bacteria and Archaea.

The first one, mostly numerous in the intestinal tract, includes many subclasses differently distributed: Bacteroidetes (23%) which includes the genus Bacteroides; Firmicutes (64%) which includes Bacillus, Clostrides and Mollicutes; Proteobacteria (8%), Gram-negative bacteria such as Escherichia coli and Helicobacter pylori; Actinobacteria (3%) which includes species such as Bifidobacterium ([24]). Among all the microorganisms present, the dominant species in the intestinal site of an adult, as mentioned above, can be included in two main groups: Bacteroidetes and Firmicutes.

BACTEROIDETES: they form about 24-25% of the intestinal microbiote and consist of about 20 genera, of which the Bacteroidales class is the one most studied, in particular the genus Bacteroides ([25]). These are Gram negative anaerobic species, with a sticky structure, non-forming spores and resistant to bile salts, with remarkable adaptive capabilities.

Thetaiotaomicron Bacteroidetes (BT) is the main component of normal intestinal bacterial flora; It has a great ability to digest polysaccharides as it has two membrane proteins that bind and import starch, 226 glycosidase (versus 98 of the man), 64 polysaccharidase (versus 1 man). BT has developed the ability to "help" the host organism to recover and use many diet carbohydrates, pulls out mucus glycans ([23]). Generally, Bacteroidetes possess a complex system to metabolize unused carbohydrates by the host organism. FIRMICUTES: The name comes from the Latin "firmus" (strong) and "cutis" (skin), they are characterized by a peptidoglycan layer that gives them a certain degree of resistance to mechanical deformation. Several species produce endospores that can survive in extreme conditions. They are Gram positive bacteria, including 250 genera and are mainly represented by Clostrides and Bacilli. Clostrides are obligatory anaerobes capable of producing endospores, if cultivated in a low-potency environment, they are extremely active in the fermentative sense: they metabolize organic substances (carbohydrates and proteins) with alcohol production, acetic acid, butyric acid, succinic acid and volatile substances such as carbon dioxide, hydrogen and hydrogen sulphide. Clostridium perfrigens, Clostridium bifermentas and Clostridium ramosum are the most common species isolated in humans.

More than 8% of adults are Clostridium difficile carriers, which can cause diarrhea, fever, pseudomembranous colitis in subjects who take antibiotics ([26]). Bacilluses, such as Clostrides, are able to produce endospores but unlike these ones they are optional or obligatory aerobic bacteria. Characterized by a typical rod shape, they include two main orders: 5 Bacillales (Bacillus, Listeria, Staphylococcus) and Lactobacillales (Enterococcus, Lactobacillus, Lactococcus, etc.). Mollicutes (from the Latin "mollis", or tender, and "cutis", cute) are instead a class of low-wall bacteria, typically 0.2-0.3 microns. The best known are Mycoplasmas. The Archaea community of the human intestinal tract is very simple and it consists of only three isolates: Methanosphaerastadtmanae, Methanobrevibacter ruminantium, and Methanobrevibacter smithii, which accounts for up to 10% of the intestinal microbiotics ([15]). The diversity of eukaryotes in the human intestinal microbiote was determined by cultivation-dependent approaches. From human

intestinal samples, 17 species belonging to the genera Candida, Aspergillus and Penicillium were isolated.

Except for Candida albicans and Rugged Candida, eukaryotes were neither widely distributed nor abundant in the human intestines (estimated to account for about 0.05% of the fecal microbial). Viruses represent a further and important constituent of the human intestinal microbiote, as indicated by recent studies that identified more than 1200 viral genotypes in the human feces with a density up to 109 virions per gram of dry material ([27]), and bacteriophage in the mucosa of healthy subjects with intestinal inflammatory diseases ([28]). Bacteriophages act a strong influence on bacterial diversity and population structure, and they are likely to be involved in disorganized phenomena, destabilizing bacterial communities ([29]).

Molecular interactions between bacteria, epithelium and mucosal immune system

The gastrointestinal tract plays an increasingly important role as a primary immunological organ. It is thus apparent that any alteration of its complex anatomic function and small intestine may alter the balance of the immune system. The intestinal mucosa of the tenuum is continually exposed to antigenic stimulation by the ingested substances and the microbial flora present in the lumen. Specific immune mechanisms allow the identification and processing of antigen, the induction of immune cellular and humoral responses, memory, tolerance regulation, and effecient system recall that are adapted to respond to the ongoing threat of injury ([30]).

The intestinal mucosa of healthy subjects is characterized by a physiological inflammatory state (determined by the continuous stimulation of the local immune system by antigens present in the lumen). The intestinal mucosa epithelium is constituted by enterocytes, globet cells, neuroendocrine cells, and hosts the so-called lymphoid tissue associated with the gut-associated lymphoid tissue (GALT). GALT consists of focal aggregates (Peyer Plates) that produce and release various antibacterial molecules such as lysozyme, α-defensine, C-type lectin, phospholipase A2 ([31]).

The Peyer Plates, in turn, are covered by a specialized epithelium (FAE) (follicle associated epiphelim) containing dendritic cells (APCs) and membrane M cells that are specialized in the transport of antigens to their own lymphocytes. Most of the immune cells, including mononuclear leukocytes (macrophages and monocytes), dendritic cells (DCs), intraepithelial lymphocytes, stromal cells, adaptive immune cells such as lymphocytes B that secrete leukocytes are found in the lamina and in the mucosa. IgA secretories and T lymphocytes.

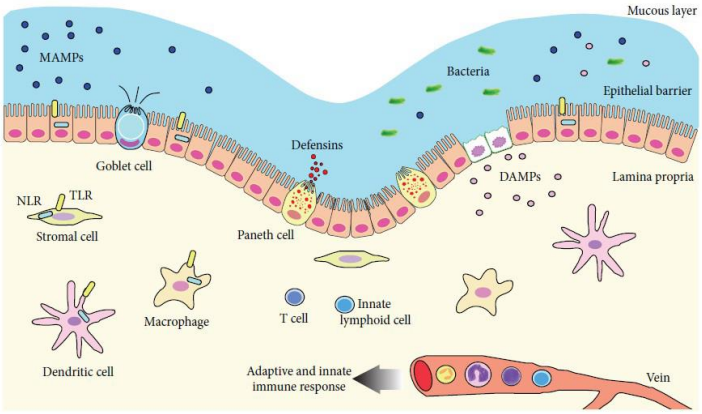

The adaptive immune system serves two fundamental elements: Th1 (T-Helper type 1) and Th2 (T-Helper type 2) lymphocytes that have significant functional differences. In the initial phase of the immune response if a Th lymphocyte encounters the antigen, particularly intracellular pathogens, in the presence of IL-12 and / or IFN-γ (interleukin-12, interferon γ) will become a type 1 (Th1) . Conversely, if an antigenic stimulus occurs in the absence of IL-12 or IFN-γ, the Th cell utilizes IL-4 produced autocrine to differentiate into a Th2 cell, which produces IL-4 and IL-10. The ability to express a different cytokine profile implies the expression of different functions (Figure 5). The core of immune efficiency and hence of individual health has its bases in the balance between Th1 and Th2.

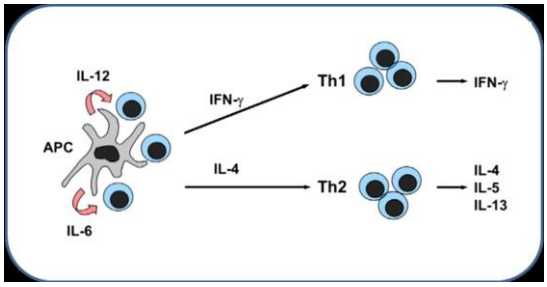

For several factors this balance may be missing by favoring an immune orientation or the other. The most important feature of dental bacteria is their interaction with the immune system: they are able to activate innate and adaptive immunity (Figure 6).

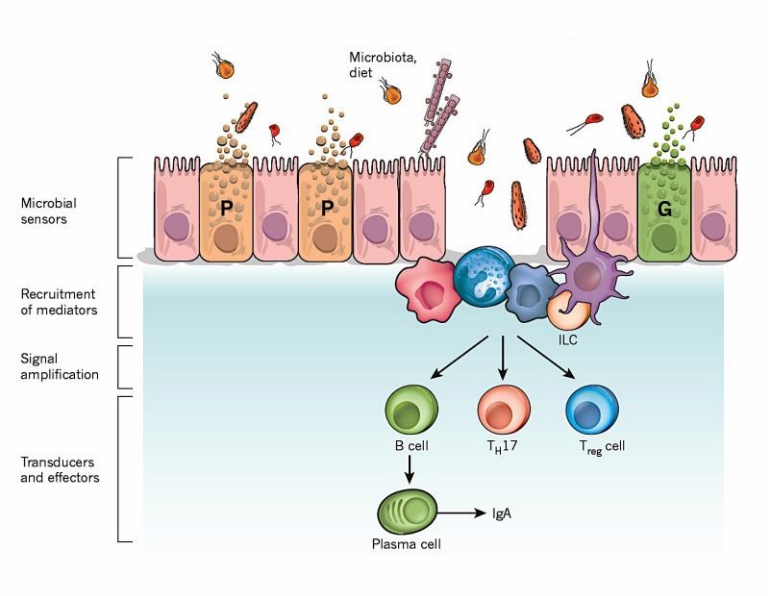

Bacterial colonization is crucial to the development and function of the immune system and helps to maintain homeostasis in the gastrointestinal tract. The intestinal mucosa represents the main interface between the immune system and the external environment, and host and bacteria collaboration seems to play a role in the development of the immune system. The crucial importance of microbiosis in the gastrointestinal tract in the development of the mucous membrane and the systemic immune system is widely documented by studies on germ-free animals ([32]). The absence of microorganisms in germ-free animals has been associated with a reduced development of the immune system compared to conventional animals. For example, germ-free mice exhibit smaller Peyer plaques ([33]), in the opposite direction they develop when germ-free animals are exposed to bacteria and are more abundant in the heifer where the number of bacteria is higher. In addition, germ-free mice have a small number of T CD4 + and immunoglobulin A cells produced by the B cells in their own lamina compared to animals with normal microbiosis ([34]). In addition, intestinal dendritic cells are less present in germ-free animals, and there is evidence for microbial role in the development of lymphocytes B. Also, intestinal bacterial signals appear to be important for the development of T-helper type 1 lymphocyte regulation and 2. There are several adaptations that regulate the symbiotic relationship between men and their intestinal microbiosis ([35]).

In a healthy bowel, these adaptations prevent a constant activation of the immune system against commensal bacteria and food antigens, while at the same time helping to protect against pathogens. Inside the colon, considering the vast increase in microbial density, the immune response is instead focused on the prevention of inflammatory response against the dental microbiot. The thickest layer of mucus in the colon, compared to that of the small intestine, provides a physical barrier to prevent bacterial entry into the epithelium. The large number of immunoglobulins A produced by plasma cells and interleukin 10 (IL-10) produced by macrophages and T cells in the colon confirm the importance of regulatory immune function within this part of the gastro-intestinal tract ([36]). There is therefore a dynamic relationship between immune and microbial systems.

Bacteria in the intestinal lumen are recognized by intestinal epithelial cells (IECs) and immune cells through the expression of receptor recognition patterns (PRRs). These receptors recognize common structures on the microbial surface, i.e. micro-associated molecular patterns (PAMPs or MAMPs), which are structures present on both pathogens and commensal microbes ([37]). The first molecule of a commensal microorganism that showed a beneficial influence on the immune response was Capsular A produced by Bacteroides fragilis. PRRs comprise several receptor families, although the best represented are TLRs and NOD-like receptors (Figure 7).

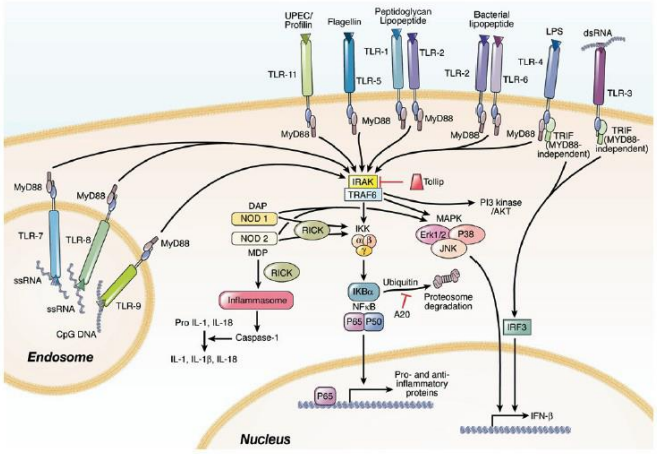

Fig. 9. Toll- e nod-like receptor (TLR e NLR).
TLR e NLR consentono il riconoscimento di ligandi batterici specifici e determinano l'attivazione di pathway di trasduzione del segnale, che coinvolgono, ad esempio, NF-kB e MAPK.

TLRs are a family of transmembrane proteins expressed above all on the surface of immunocompetent cells, ie monocytes, macrophages and dendritic cells, but also on the surface of epithelial cells ([38]). Some of the thirteen TLRs found today in mice and humans are located in cell membranes, others in endosomal membranes, to recognize distinct extracellular and endocellular MAMPs, respectively, causing the activation of different signal pathways ([37]). TLR2, 4, 5 and 9 recognize common bacterial and fungi structures, while TLR3, 7 and 8 are mainly involved in viral detection. An important example of MAMP is lipopolysaccharide (LPS), which represents an important part of the cell wall of Gram-negative bacteria, such as Proteobacteria, which stimulates TLR4. Other examples are the peptidoglycan found in the wall of Gram-positive bacteria and the flagellin produced by scattered bacteria which induce the stimulation of TLR2 ([40]) and TLR5 ([41]). TLR stimulation triggers a downfall of signals leading to activation of NF-κB transcription factor, and JNK and MAP (mitogenactivated protein kinases) kinases. This signal cascade causes the release of proinflammatory cytokines and chemochins, resulting in the initiation of an inflammatory response to pathogens. Since the TLR signal is critical in the innate defense against pathogens, the constant activation of the immune system of the gastro-intestinal tract for the recognition of the residual microbiotic would be pathological.

For this reason, the host must be able to distinguish between diners and pathogens and balance immunity and tolerance. It has been hypothesized that lack of inflammation in response to microflora is feasible as commensional bacterial products stimulate TLRs and trigger signaling leading to the production of cytoprotective factors, such as IL-6 and IL-10 interleukins, and tumor

necrosis factor (TNF) -α, which play a crucial role in maintaining the homeostasis of the intestinal epithelium ([42]). In addition, immunity tolerance is achieved by regulating the expression and distribution of PRRs in the gastrointestinal tract ([37]). For example, IECs express low levels of TLR2 and TLR4 in health conditions, reflecting one of the underlying mechanisms of low immune responses to dental bacteria ([43,44]). Differences in the expression of PRRs between the apical and basalateral surface of the IECs represent another way to distinguish pathogenic bacteria from the dinosaurs ([45]). Despite these mechanisms to reduce the TLR signal in the healthy intestine, it is increasingly evident that a basal TLR signal induced by the luminous microbial contributes to homeostasis ([37]). Recent studies have shown a more complex role for the IEC than the simple formation of a physical barrier between the lumen and the underlying tissue, as intestinal epithelial cells retain immune homeostasis by perceiving the surrounding microbial environment through expression of PRRs and the subsequent regulation of cell function of antigen and lymphocytes ([46,47]).

The function of the IEC is strongly influenced by the commensal bacteria, which are able to modulate the signal of these cells actively ([48]). This modulation provides a mechanism for dental bacteria so as to be recognized by the IECs without activating a pro-inflammatory immune response. Some obese bacteria can directly inhibit the activation of Nf-kB ([36]). Under stationary conditions, this transcription factor is linked to its IkB inhibitor, which prevents its nuclear translocation. The classic Nf-kB activation, following receptor stimulation, is obtained by the phosphorylation, ubiquitination and proteasomal degradation of IkB, resulting in the Nf-kB translocation within the nucleus, where it activates the inflammatory cytokine transcription and chemokines ([49]). Experiments with non-virulent Salmonella strains showed that these dendritic bacteria inhibit the ubiquitination pathway and subsequent degradation of IkB, thus preventing the activation of Nf-kB and maintain a low epithelial response to the luminous microbial ([41]). Also the metabolites derived from the dental bacteria are known as modulators of the innate immune response, providing another mechanism for maintaining intestinal immune and homeostasis and tolerance. An example is given by butyrate, a short chain of fatty acids and one of the main end products of fermentation of dietary fiber by intestinal bacteria, which represents the largest source of energy for the IEC, but can directly exert immunomodulatory and anti- inflammatory. Butyrate inhibits the activity of the dehydrogenase and thus suppresses the proteasomal activity by reducing the expression levels of some proteasome subunits. This results in inhibiting the proteasomal degradation of IkB and therefore limits the activation of Nf-kB. In addition, IEC recognition of the bacterial bones leads to the production of several immunoregulatory molecules, for example TSLP and the transforming beta growth factor (TGF-β) ([50]). Acetate, too, can exert important immunomodulatory effects by suppressing the activation of the κB nuclear factor and / or by acting on G coupled receptors.

These signals, one at a time, promote the development of mucosal immune cells with tollerogenic properties. This cross-talk between commensal bacteria, IEC and immune cells is important for the maintenance of homeostasis and the containment of uncontrolled inflammation in the gastrointestinal tract ([50]). In the intestinal mucosa the activation of reconnaissance receptors begins the pathway of the nuclear factor κB, protein kinases and caspases, triggering a signal

cascade. This leads to the production and release of protective peptides, cytokines, chemokines and phagocytes. All this results in a protective response from dental bacteria, an inflammatory response to pathogenic organisms, or the apoptosis trigger. As for NOD-like receptors (NLRs), they mediate innate immunity primarily towards intracellular microorganisms and are able to recognize and bind various exogenous bacterial components such as toxins, but in principle link the molecular profiles associated with the damage (DAMPs). The NLRs family includes more than twenty cytosolic receptors in the mammals, mainly divided into two categories, NOD1 and NOD2, based on the N-terminal domain structure involved in the signal transduction. NLR stimulation triggers the activation of caspase and NF-κB transcription factor downstream, resulting in inflammatory mediators, defensing and regulating apoptotic signals with dysfunction of the autophagy process. Another receptor class, G protein-coupled receptors, can bind short-chain fatty acids (SCFAs) produced by the intestinal microbial, particularly Bacteroidetes and Firmicutes after fermentation of dietary fibers. This class of receptors consists of three subgroups defined as GRP41, GRP43 and GPR109A, which mediate different signals such as epithelial cell proliferation, differentiation, gene expression, and anti-inflammatory effects on the mucosa. Tolerance against commensal bacterial antigens is also ensured by the presence of a specialized subpopulation of T or T suppressor T lymphocytes expressing membrane glycoproteins such as CD8, CD4, CD35 and Foxp3 (transcription factor essential for differentiation to Treg).

Regulatory lymphocytes suppress the effective responses of other cells by the production of inhibitory cytokines such as IL-10 and TGF-β following activation by some commensal bacteria such as Bacteroidetes and Clostridium, clusters IV and XI, Foxp3 expression by producing bacterial metabolites such as fatty acids (57). Given the numerical complexity of the intestinal microbial it is inevitable that some of the dinosaur microorganisms can cross the epithelial barrier and access their own lamina, where they are phagocytised and destroyed by intestinal macrophages; in parallel, M2 subtype macrophages induce proliferation of epithelial progenitor cells to regenerate damaged epithelium. Other mechanisms that are used by epithelial cells to minimize contact with intestinal bacteria are secretion of antibacterial peptides (AMPs), bacteriostats such as catepsin, lipocaline-2, and lectin Reg3. In addition, there are numerous experimental evidence on the ability of dendritic cells (DCs) once contacted with the bacterial antigen to stimulate and induce differentiation of lymphocytes B resulting in IgA production specific for the benthic bacteria ([51]) . Antimicrobial immunoglobulins are captured by epithelial cells and translocated on the apical surface of the epithelium where they bind to dental bacteria, limiting their ability to penetrate the epithelial barrier. Therefore, gastrointestinal tract bacteria play an active role in the development and homeostasis of the immune system. In addition, while potentially pathogenic bacteria have a monomorphic aspect, dental organisms are able to change continuously by contributing to host immune surveillance and maintaining a predominant ecological niche in the intestinal tract ([52])

An increasing number of studies have shown that a diversified and balanced composition of the microbiota is crucial for the development and well-being of the individual. An alteration of bacterial flora both qualitatively and quantitatively is called "dysbiosis". This is responsible for the onset of local and systemic alterations that play an important pathogenetic role not only in inflammatory and functional bowel disorders but may affect any organs and organs of the

organism. Debiosis is associated with a wide range of disorders. Among them, diarrhea, irritable bowel syndrome (IBS), chronic bowel disease (IBD), colorectal cancer and some liver disease and allergies, as well as food-related illnesses such as obesity, type 2 diabetes or celiac disease. The composition of the intestinal microbiotics also has effects on the central nervous system because the intestines and the brain are connected by a multitude of communication pathways used by bacterial transmitters and metabolites. It is not surprising, therefore, that mental disorders and neurological development such as depression, anxiety and autism can be related to intestinal dysliosis. There are several factors that can affect the intestinal ecosystem. As already seen, the composition of flora has been largely influenced since birth. With age advancing, the change in the microbiota becomes more apparent due to several factors such as diet change, appearance of diseases, possible antibiotic treatments, and immune system modification. The crucial question of the causal links between debiosis and associated diseases, however, remains unclear, and it is hypothesized that some microbial alterations may be considered the result of the pathogenic process or be the cause of the disease. Table 1 summarizes some pathogenetic mechanisms through which the intestinal microbial is able to intervene in the genesis of various pathologies (60)

Patients and Methods

CARAMEL (Clinic**A**l prognostic biomarkers for Ipilimumab-**R**el**A**ted outcome in metastatic **MEL**anoma patients**) Study Design**

The study is a multicentric retrospective observational Study, collecting data from 120 patients enrolled in several national cancer institutes: Oncology Unit of the AOU of Pisa, Oncology Unit of Businco Hospital (Cagliari), Oncology Unit of SS. Annunziata Hospital (Chieti), Oncology Unit of Macerata Hospital of, the Oncology Unit of IRCCS of Bari, Oncology Unit of the National Cancer Institute of Milan and the Oncology Unit of the University Hospital of Cagliari.

Patients enrolled in the study presented the following inclusion criteria:
- Histologic diagnosis of metastatic melanoma treated with Ipilimumab as I, II or III line after previous therapies failure (chemotherapy and molecular target therapies);
- Measurable metastatic lesions (> 1 cm) according to RECIST v 1.1;
- Older than 18 years of age;
- Life expectancy of at least 4 months.

Exclusion criteria were:
- Diagnosis of concomitant autoimmune disease in the active phase;
- Pregnancy or concomitant episode of thyroiditis or pituitary gland;
- Increased risk of concomitant gastrointestinal bleeding following an anticoagulant treatment;
- Presence of symptomatic cerebral metastases or requiring therapy with steroids high dosage;
- Serological positivity for Hepatitis B and C and HIV viruses;
- Baseline AST> 2.5 x LSN values and total bilirubin values at baseline ≥ 3 x LSN;
- Pregnancy and lactation for female patients;
- Impossibility for verbal and written consent to informed consent.

Patients were enrolled in the period between January 2013 and January 2016 and received Ipilimumab as indicated on the technical sheet, in monotherapy at a dose of 3 mg / kg administered intravenously every 3 weeks, for a total of 4 doses.
Patients enrolled in the study received Ipilimumab within the ExpandedAccess Program (EAP) or as an indication in the front line after approval of the Italian Medicines Agency (AIFA), in September 2014.
After obtaining the results of this cohort, we performed a validation of the data with a further validation cohort, namely 20 patients enrolled in the center of the Genoa Cancer Institute.

CREAM (Clinical correlation between immunotherapy-**RE**lated colitis **A**nd intestinal **M**icrobiote**) Study Design**

The study is a multicentric observational Study, collecting data from 20 patients enrolled in Sardinian Hospitals: Oncology Unit of NS Mercede Hospital (Lanusei), Oncology Unit of the University Hospital of Cagliari, Oncology Unit of S. Marcellino Hospital (Muravera), Oncology Unit of Businco Hospital (Cagliari).

Patients enrolled in the study presented the following inclusion criteria:
- Histologic diagnosis of metastatic melanoma, NSCLC, RCC or H&N treated with Ipilimumab, Nivolumab or Pembrolizumab as I, II or III line after previous therapies failure;
- Measurable metastatic lesions (> 1 cm) according to RECIST v 1.1;
- Older than 18 years of age;
- Life expectancy of at least 4 months.

Exclusion criteria were:
- Diagnosis of concomitant autoimmune disease in the active phase;
- Pregnancy or concomitant episode of thyroiditis or pituitary gland;
- Increased risk of concomitant gastrointestinal bleeding following an anticoagulant treatment;
- Presence of symptomatic cerebral metastases or requiring therapy with steroids high dosage;
- Serological positivity for Hepatitis B and C and HIV viruses;
- Baseline AST> 2.5 x LSN values and total bilirubin values at baseline ≥ 3 x LSN;
- Pregnancy and lactation for female patients;
- Impossibility for verbal and written consent to informed consent.

Patients were enrolled in the period between January 2016 and October 2017 and received Ipilimumab in monotherapy at a dose of 3 mg / kg administered intravenously every 3 weeks, for a total of 4 doses; Nivolumab at a dose of 3 mg /kg administered intravenously every 2 weeks until progression disease or unacceptable toxicity; Pembrolizumab at a dose of 2 mg /kg administered intravenously every 3 weeks until progression disease or unacceptable toxicity.

COFFEE (Clinical pr**O**gnostic biomarkers e**FF**ective for immunotherapy-r**E**lated outcom**E** in solid tumors**) Study Design**

The study is a multicentric observational Study, collecting data from 39 patients enrolled in Sardinian Hospitals: Oncology Unit of NS Mercede Hospital (Lanusei), Oncology Unit of the University Hospital of Cagliari, Oncology Unit of S. Marcellino Hospital (Muravera), Oncology Unit of Businco Hospital (Cagliari).

Patients enrolled in the study presented the following inclusion criteria:
- Histologic diagnosis of metastatic melanoma, NSCLC, RCC or H&N treated with Ipilimumab, Nivolumab or Pembrolizumab as I, II or III line after previous therapies failure;
- Measurable metastatic lesions (> 1 cm) according to RECIST v 1.1;
- Older than 18 years of age;
- Life expectancy of at least 4 months.

Exclusion criteria were:
- Diagnosis of concomitant autoimmune disease in the active phase;
- Pregnancy or concomitant episode of thyroiditis or pituitary gland;
- Increased risk of concomitant gastrointestinal bleeding following an anticoagulant treatment;
- Presence of symptomatic cerebral metastases or requiring therapy with steroids high dosage;
- Serological positivity for Hepatitis B and C and HIV viruses;
- Baseline AST> 2.5 x LSN values and total bilirubin values at baseline ≥ 3 x LSN;
- Pregnancy and lactation for female patients;
- Impossibility for verbal and written consent to informed consent.

Patients were enrolled in the period between January 2016 and October 2017 and received Ipilimumab in monotherapy at a dose of 3 mg / kg administered intravenously every 3 weeks, for a total of 4 doses; Nivolumab at a dose of 3 mg /kg administered intravenously every 2 weeks until progression disease or unacceptable toxicity; Pembrolizumab at a dose of 2 mg /kg administered intravenously every 3 weeks until progression disease or unacceptable toxicity.

Parameters evaluated

For CARAMEL and COFFEE studies The clinical parameters considered were:
- Sex (male / female);
- Number of metastatic disease sites (less than three sites / more than three sites);
- Mutational status of BRAF (wild type / mutated);
- Age (<or> 65 years).

The laboratory parameters considered are as follows:
- Absolute number of neutrophils;
- Absolute number of lymphocytes;
- Absolute number of eosinophils;
- Platelets count;
- Lacticodeidrogenase (LDH) serum dosage;
- Neutrophil / lymphocyte ratio;
- Platelet / lymphocyte ratio;
- Neutrophil / eosinophil ratio;
- Platelet / eosinophil ratio.

All parameters referred to baseline values, before starting treatment.
The cut-off values of our parameters were identified by ROC analysis (Receiver Operating Characteristics).

As regards the CREAM study, a sample of fecal material was taken before starting the treatment and, subsequently, after two months (so after three administrations of Pembrolizumab or after four doses of Nivolumab).

Clinical Parameters

The collected clinical data included age, sex, primary tumor site, histological type, molecular classification, staging at the diagnosis time, the timing of the metastatic disease and metastatic sites.

Tumor response evaluations were conducted after the Completion of scheduled cycles as regards Ipilimumab, and every three administrations of Pembrolizumab or every four administrations of Nivolumab. Instrumental re-evaluations have been performed by CT scan of head an total body and / or tomoscintigraphy global body (PET) with 18-FDG.

In case of partial / complete response or Stability of the disease TC controls were performed later every three months.

In all patients, data on progression free survival and overall survival were collected. The objective responses intended as a response complete (CR) or partial response (PR) were evaluated according to RECIST criteria (Solid Tumor Response Evaluation Criteria) v.1.1 [61].

Statistical analysis

The overall survival rate was performed by Kaplan- Meier and it was calculated by considering the time between the first administration of immune therapy to the date of death from any cause (for patients lost at follow up we considered the last contact).

Progression free survival evaluation was evaluated with the same system, indicating the progression as the end of the observation clinical period/radiological disease.

The predictive value was calculated in terms of probability of survival among the various groups by log-rank test. The correlation analysis was performed by univariate regression analysis. Multivariate analysis was performed to rule out any spurious associations between the factors considered, by only analyzing those factors that were statistically significant correlated to the OS and the PFS to univariate analysis.

All statistical analyzes relating to survival or correlation with individuals variables, except those otherwise specified, have been performed using GraphPad 6 Prism Software. Multivariate analysis was conducted with the SPSS Software v.15.

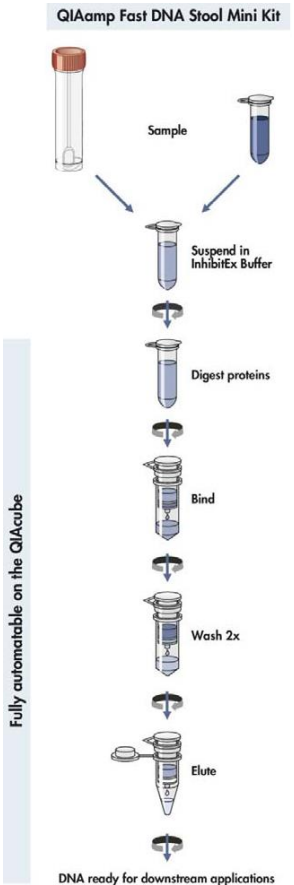

Extraction of genomic DNA from stool

Total genomic DNA was extracted from each stool sample using the QIAamp Fast DNA Stool Mini Kit. About 180-200 mg of stool were resuspended in 1 ml of Inhibitor Buffer and incubated for 5 minutes at 70 ° C in Thermoblock. The homogenate was then centrifuged at 14,000 rpm for 1 minute and 200 µl of supernatant obtained was transferred to microtubule tubes containing 15 µl of Proteinase K. 200 µl of Buffer AL were then added and after homogeneous solution by Vortex and incubated for further 10 minutes at 70 ° C.

At the end of this step, the samples were supplemented with 200 µl of 100% ethanol. The material contained in each microcentrifuge tube constituted at this extraction stage of 600 µl of lysate was completely transferred to special centrifuge columns (QIAamp Column) and centrifuged at 14,000 rpm for 1 minute.

The obtained material, once adhered to the centrifuge column silica gel, undergoes two consecutive wash cycles by means of two different washing pads named 53 AW1 and AW2. Finally, after addition of 200 µl of elution buffer ATE, each QIAamp Column is centrifuged at 14,000 rpm for 1 minute. The eluate thus obtained, consisting of total genomic DNA, was stored at a temperature of -20 ° C until the subsequent analytical procedures were performed.

Quantitative DNA analysis was performed by spectrophotometric reading with NanoDrop ND-1000 by measuring the absorbance of the sample at a wavelength of 260 nm. Sample purity was evaluated by analyzing the ratios of absorbance values (260/280 and 260/230) in combination with overall spectral quality.

Polymerase Chain Reaction (PCR)

The next step was to amplify the bacterial DNA of each sample of each patient. Couples of group-specific primers were used, each of which complementing specific regions of the 16S ribosomal distinctive of each taxonomic group. A pair of primers has also been used for a preserved 16S region capable of amplifying "Universal" bacterial gene sequences.

Target	Primer sequences
Bacteroides-Prevotella-Porphyromonas	BFRAF: 5'-GGTGTCGGCTTAAGTGCCAT-3' BIFRAR: 5'-CGGA(C/T)GTAAGGGCCGTGC-3'
Bifidobacterium spp.	BIFF: 5'-GCGTGCTTAACACATGCAAGTC-3' BIFR: 5'-CACCCGTTTCCAGGAGCTATT-3'
Lactobacillus	LBF: 5'-AGCAGTAGGGAATCTTCCA-3' LBR: 5'-CACCGCTACACATGGAG-3'
Universal Bacteria	UBF: 5'ACTCCTACGGGAGGCAG-3' UBR: 5'-GACTACCAGGGTATCTAATCC-3'

Table 1: Target and respective primer sequences

The PCR reaction was assessed in a microcentrifuge tube according to the following protocol: 5 µl of 10X PCR Buffer, 1 µl of $MgCl_2$ 50 mM, 1 µl of 10 mM dNTPs, 1 µl of Forward Primer 10 µM, 1 µl of Reverse Primer 10 µM, 0.2 µl Taq DNA Polymerase 5U/µl and 10 µl of genomic DNA. The reaction mixture was then brought to a final volume of 50 µl with DEPC water. 55 DNA amplification was performed using the Applied Biosystem 9700 thermocycler. In particular, the samples were subjected to 95 °C for 5 minutes (initial denaturation); Subsequently, the amplification reaction was carried out for 35 cycles: DNA denaturation at 95 °C for 15 seconds, annealing of primers at 52 °C for 20 seconds, extension of DNA at 72 °C for 45". Finally, a terminal extension phase was carried out at 72 °C for 5 minutes and a final refrigeration at 4 °C. The amplification products were visualized by running on agarose gel at 2% and staining with SYBR Safe and then analyzed by ultraviolet light transilluminator to show the bp correspondence of the amplified fragment.

Quantitative analysis by Real-Time PCR

Total DNA obtained after extraction was quantified by PCR Real Time technique. Complementary oligonucleotide sequences, upstream and downstream regions of V3 and V4 regions of ribosomal 16S gene, were used as primers. The sequences of the primers used in the reaction are shown below:

16S F2 (Forward Primer): 5'-CCTACGGGNGGCWGCAG-3'
16S R2 (Reverse Primer): 5'-GACTACHVGGGTATCTAATCC-3'

Quantitative results were obtained by interpolating values with those obtained from a standard curve using the E. coli genomic DNA previously extracted from pure colony by using the QIAamp DNA Mini Kit (Qiagen) kit. The extracted E. coli genomic DNA was quantitated by spectrophotometric reading with the NanoDrop1000 instrument and serial dilutions were made to obtain final concentrations of 7.5ng, 0.75ng, 0.075ng and 0.0075ng of DN. A standard curve was thus constructed by detecting fluorescence and constructing the linear regression line as shown in **Figure 1**. As a fluorescence marker, SYBR Green (Qiagen) and reaction mix consisted of a final volume of 20µl for each sample consisting of: 10µl of SYBR Green PCR SuperMix, 0.5µl of 16S F2 10 µM, 0.5µl of $16S_2O$ 10 µM, 5µl of genomic DNA and 4µl of DEPC water.
The amplification (**Figure 2**) was carried out using the CFX96 Touch Real-Time PCR Detection System (Bio-Rad) instrument with the following profile: 3 minutes at 98 °C for Taq Polymerase activation and repeating for 33 cycles of the next two phases at 98 °C for 15" (denaturation) and 59 °C for 50" (annealing-extension).

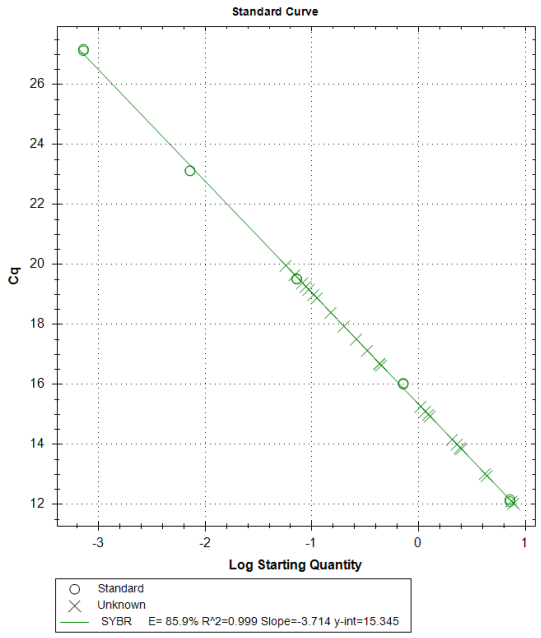

Figure 1

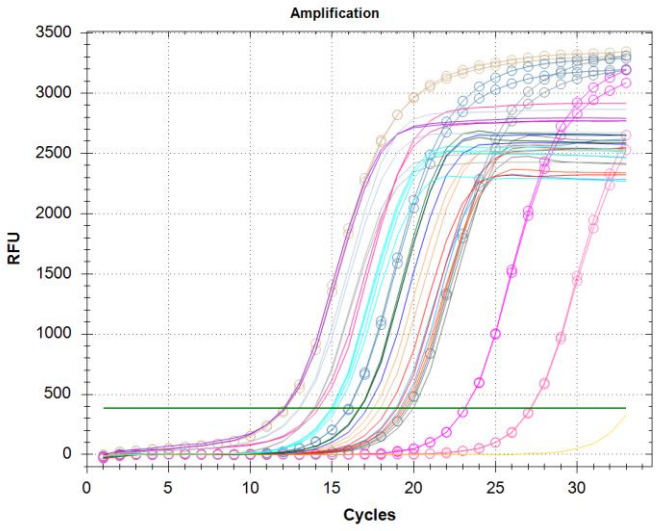

Figure 2

Sequencing

The NGS MiSeq platform (Illumina) provides an operational workflow consisting of four main phases: template preparation, cluster generation, sequencing and imaging, bioinformatics analysis of data.

Template setup

Clone library 16S amplification

Metagenomics studies are commonly performed by analyzing the region 16S of the ribosomal RNA of the prokaryotes. The first step in the template preparation phase is to amplify V3 and V4 regions of the rRNA gene 16S to obtain millions of identical copies (clones) of the molecules that make up the library. Because NGS instruments do not have image data analysis systems capable of detecting single fluorescence emissions, they require pre-amplification of the templates so that the fluorescence signal is sufficiently intense to be detected by the instrument. The clone amplification phase of the 16S libraries involves insertion at the ends of each molecule of the genomic library of known sequence sequence defined oligonucleotides adapting regions that will serve for the insertion of Illumina Indexes and adapters used in the subsequent steps of template preparation. This process can be accomplished by PCR reaction since the adaptive regions are part of the nucleotide sequence of specific primers used in the reaction (**Figure 3**): in addition to being complementary to the upstream and downstream regions of the regions from amplify, have a protruding sequence formed by the adapting regions (underlined) as follows:

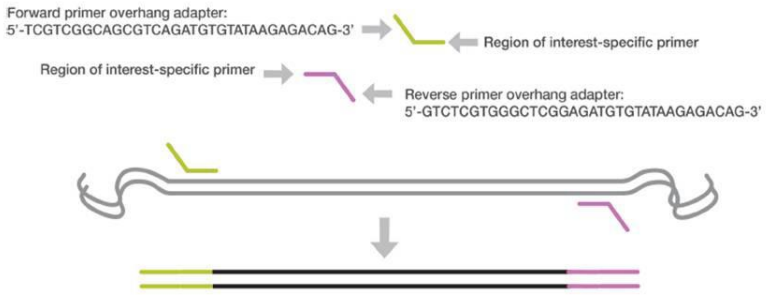

Figure 3: *Template of insertion of genomic DNA*

The clone amplification phase of the 16S libraries involves the insertion at the ends of each molecule of the genomic library of known oligonucleotides sequences, better known as adapting regions, that will serve for the insertion of Illumina Indexes and adapters used in the subsequent steps of template preparation. This process can be accomplished by PCR reaction since the adaptive regions are part of the nucleotide sequence of specific primers used in the reaction (**Figure 3**): in addition to be complementary to the upstream and downstream regions of the regions to be amplified, they have a protruding sequence formed by the adapting regions (underlined) as follows:

16S Forward Primer = 5'-3'

TCGTCGGCAGCGTCAGATGTGTATAAGAGACAGCCTACGGGNGGCWGCAG

16S Reverse Primer = 5'-3'

GTCTCGTGGGCTCGGAGATGTGTATAAGAGACAGGACTACHVGGGTATCTAATCC

The PCR reaction was prepared using the following profile: 5 µl of 10X PCR Buffer, 1.5 µl of $MgSO_4$ 50 mM, 1 µl of 10 mM dNTPs, 1 µl of Forward Primer 10 µM, 1 µl of Reverse Primer 10 µM, 0.2 µl of Taq DNA Polymerase 5U / µl and 12.5 µg of genomic DNA. Each mix of reaction was brought to a final volume of 50 µl with DEPC water. DNA amplification was accomplished using the Applied Biosystem 9700 thermocycler. In particular, the samples were subjected to 95 °C for 3 minutes; Subsequently, the amplification reaction was carried out for 35 cycles: DNA denaturation at 95 ° C for 30 seconds, annealing of primers at 52 °C for 30 seconds, extension of DNA at 72 °C for 30 seconds. Finally, a terminal extension phase was carried out at 72 °C for 5 minutes and a final refrigeration at 4 °C. The amplification products were run on 2% agarose gel interlaced by SYBR Safe and displayed to the ultraviolet light transilluminator.

Purification of PCR products

The PCR products were subsequently purified using AMPure XP beads. This step separates the amplified material from the free primers and the primary dimers present in the reaction. The samples were centrifuged at 1000g at 20 ° C for 1 minute, resuspended with 20 µl of AMPure XP

marbles and incubated at room temperature for 5 minutes. At the end of the incubation, the multiwell containing the samples was placed over a magnetic rack for 2 minutes. The obtained supernatant was removed and the sample passed twice in 200 µl of 80% ethanol. After removing the supernatant, the remaining ethanol now in the magnetic beads was allowed to evaporate in air for 10 minutes. Subsequently, all samples were incubated for 2 minutes with 52.5 µl of 10 mM Tris pH 8.5, with a further two-minute incubation of the multi-well inserted into their magnetic rack. Finally, 50 µl of supernatant of each sample was taken and aliquoted into a new multi-well container.

Indexing the Library 16S

Il secondo step di PCR è stato eseguito sul prodotto di amplificazione purificato derivante dalla prima PCR, al fine di indicizzare i diversi campioni ed inserire gli adattatori di sequenziamento (Figura 21). In questa fase avviene una vera e propria marcatura del DNA attraverso l'utilizzo delle sequenze indice che fungono da barcode. Questo requisito è indispensabile affinché rimanga un'identificazione univoca di ogni campione nel processo di pooling.

La funzione degli adattatori è quella di ancorarsi ad oligonucleotidi a loro complementari presenti sulla superficie della flow-cell di sequenziamento. Gli indici duplici e gli adattatori di sequenziamento sono stati uniti alla libreria mediante l'utilizzo del kit commerciale Nextera XT Index Kit (Illumina). In particolare sono state utilizzate coppie di indici di otto basi ciascuna, Nextera XT Index 1 (i7) adiacente alla sequenza dell'adattatore P7 e Nextera XT Index 2 (i5) adiacente alla sequenza dell'adattatore P5. La Nextera XT Index Kit per 96 campioni utilizza 12 differenti Index 1 e 8 differenti Index 2 (Tab. 6). La combinazione dei diversi tipi di Index 1 e 2 ha permesso di indicizzare un totale di 96 campioni.

The second step of PCR was performed on the purified amplification product derived from the first PCR in order to index the different samples and insert the sequencing adapters (**Figure 4**). In this phase, a real DNA mark is made using the index sequences that act as barcode. This requirement is indispensable for a unique identification of each sample in the pooling process.

The function of the adapters is to anchor to their complementary oligonucleotides present on the surface of the sequencing flow-cell. Duplicate indexes and sequencing adapters have been combined with the library by using the Nextera XT Index Kit (Illumina) kit. In particular, eight pairs of indices of eight bases were used, Nextera XT Index 1 (i7) adjacent to the sequence of Adapter P7 and Nextera XT Index 2 (i5) adjacent to the P5 adapter sequence.

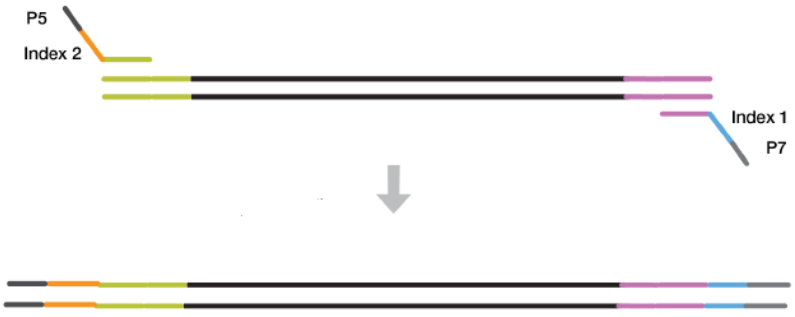

Figure 4. Indexing of DNA template sequences

Subsequently, the PCR reaction was prepared according to the following protocol: 5 µl purified DNA with AMPure XP beads, 5 µl Nextera XT Index Primer 1, 5 µl Nextera XT Index Primer 2, 25 µl 2x KAPA HiFi HotStart ReadyMix and 10 µl water DEPC. The 96-well plate was centrifuged at 1000 xga 20 ° C for one minute and then the PCR reaction was started using the Applied Biosystem 9700 temocycler according to the following amplification profile: 95 ° C for 3 minutes and 8 three phase amplification cycles at 95 ° C for 30 seconds, 55 ° C for 30 seconds, 72 ° C for 30 seconds. Finally, a phase at 72 ° C for 30 seconds followed by cooling to 4 ° C.

Purification of PCR products

Similar to what happened at the end of the PCR for the assembly of the adapters, in this case the PCR products must be purified by any contaminants present in the reaction. The protocol below is almost the same as the one before and it is different only as regards the amount of reagents used. The index PCR plate was centrifuged at 280 x g at 20 ° C for one minute. Each sample was resuspended with 56 µl of AMPure XP marbles and incubated at room temperature for 5 minutes. The multi-well containing samples were then placed over the magnetic rack for two minutes and at the end the supernatant was eliminated. Each sample was washed twine in 200 µl of 80%ethanol and after removing the supernatant, the remaining ethanol adhered to the magnetic beads was allowed to evaporate in air for 10 minutes. Subsequently, all samples were incubated for 2 minutes with 52.5 µl of 10 mM Tris pH 8.5. The multi-well was inserted into the magnetic rack and after two minutes 25 µl of supernatant and aliquoted in the wells of a new multi-well was taken. To estimate the size of the resulting libraries, the samples were diluted 1:50 and analyzed using the Agilent Technologies 2100 Bioanalyzer.

Quantifying, standardizing, and pooling libraries

The concentration of each library was checked with Qubit® 2.0 Fluorometer (Life Technologies, Carlsbad, CA). To obtain the correct concentration for mass sequencing with MiSeq technology, the molarity of each library was calculated as follows:

$$\frac{\text{(DNA library concentration -ng/µl)}}{\text{(660 g/mol x library length}} \times 10^6 = \text{DNA library concentration -nM}$$

Subsequently, genomic libraries were normalized by diluting each of them with a Tris pH 8.5 (10 mM) in order to obtain a final concentration of 4 nM per library. Finally, 5 µLdi DNA of each library was aliquoted and the aliquots were combined to form a single pool of genomic libraries.

Denaturation and dilution of libraries

Before proceeding with cluster generation and sequencing, library denaturation was performed: for this purpose, 5 µl of library was resuspended with 5 µl of NaOH at 0.2 N. After homogenizing the solution by Vortex, our sample was centrifuged at 280 xga 20 °C for one minute. Subsequently, the samples were incubated for 5 minutes at room temperature to allow DNA denaturation of the libraries. At the end of this step, the denatured libraries were diluted with 990µl of HT1 hybridization buffer to obtain a final concentration at 20pM concentration. Subsequently, the sample was further diluted to 8pM by resuspending 240 µl of the library with 360 µl of HT1 hybridization buffer.

Dilution and dilution of PhiX control

To evaluate the proper execution of the sequencing, a positive PhiX v3 control was used. The first step in the preparation phase of the control is its dilution, we added to 2 µl of PhiX library (10 nM) 3 µl Tris 10 mM at pH 8.5 to obtain a final concentration of 4 nM. 5 µl of positive control was added 5 µl of NaOH to 0.2N. After homogenizing the solution by Vortex, the sample was incubated at 96 ° C for 5 minutes to obtain heat denaturation of the control libraries. At this point, 990 µL of Hybridization Buffer HT1 frozen to the tube containing the PhiX library was added to reach a final concentration of 20 pM. Subsequently, 240 µl of the denatured library of the PhiX v3 control was resuspended in 360 µl of HT1 hybridization buffer to reach the final concentration of 8 pM equivalent to that of the sample library. Finally, the two newly denatured and diluted libraries were combined in a single tube containing: 30 µL of PhiX library and 570 µL of the genomic library obtained from DNA to be sequenced. Immediately before loading the library on the MiSeq platform, heat was denatured with heat: the library containing solution was incubated at 96 ° C for 2 minutes; at the end of the incubation, the tube was shaken by inversion 1-2 times and immediately placed on ice for 5 minutes. The prepared library was loaded onto the MiSeq cartridge, containing the reagents. The disposable cartridge provided by MiSeq Reagent Kit v3 was used, which consists of several sealed prefilled wells with the reagents needed for sequencing (**Figure 5**).

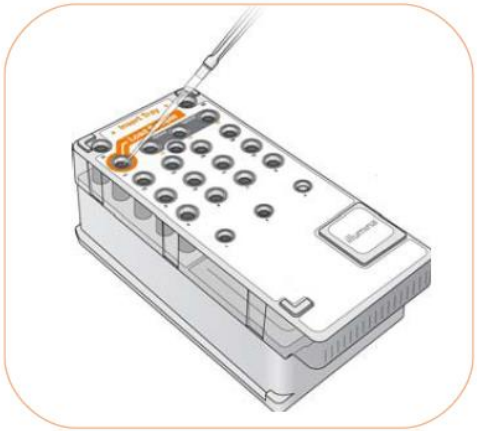

Figure 5. Loading libraries

Uploading sample libraries

Once the reagent cartridge is completely defrosted and ready for use, the libraries can be loaded into the cartridge: using the tip of a clean pipette the seal covering the tank marked with Load Samples is drilled and 600 µl of pipette in the cartridge gallery.

Cluster generation

Templates are introduced into the flow-cell plate (**Figure 6**) of the Illuminated System on whose surface two different oligonucleotides are immobilized. On the plate hybridization occurs between the template adapters and their complementary oligonucleotides.

Figure 6. Plate flow-cell Illumina

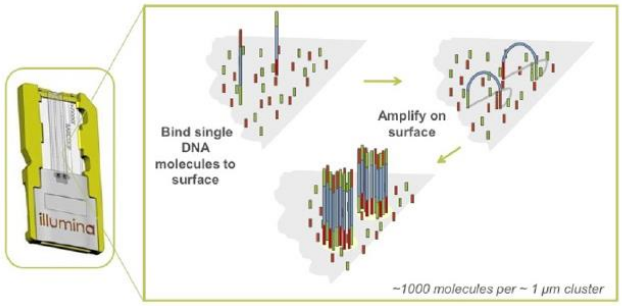

Figure 7. Template binding and cluster setup

After the template is immobilized, the extension process can start and DNA polymerase can synthesize complementary filaments to templates. The obtained molecules are denatured and the original filament is washed out of the system while the new synthesized filament, which remains bound to the plate, bends until bonded to the other end to its complementary oligonucleotide on the plate, assuming a "bridge shape"(**Figure 7**).
The bridged fragments are then amplified; a subsequent denaturation makes the fragments free from one end that folds again to bind to the adjacent complementary oligonucleotide of the plate. The operation cyclically repeats and the immobilization-synthesis-denaturation steps continue until a cluster of thousands fragments, tied to one end to the substrate, and harvested in a very limited space. The process is called bridge-PCR amplification.

Sequencing using MiSeq (Illumina)

Sequencing was performed using Illumina MiSeq platform. The clusters of each cluster align the sequencing primer that allows the start of the true sequencing reaction (**Figure 8**). Each sequencing cycle involves a DNA polymerase and dNTP reversible terminators marked with four different fluorescence molecules, one for each DNA base. Reversible terminators have the ability

to be chemically reported to the original nucleotide structure (**Figure 9**). After each incorporation, a laser excites the fluorescent dNTP terminator marker by generating a light emission that allows the base identification. The fluorescent molecule is then removed and the terminator is chemically transformed by reactivating the synthesis that allows sequencing of the subsequent base. The Illumina MiSeq platform can produce up to 15 gigabytes of data in a single run, 25 million "reads" each with a length of 2 × 300 bp each, ensuring a high degree precision and reliability.

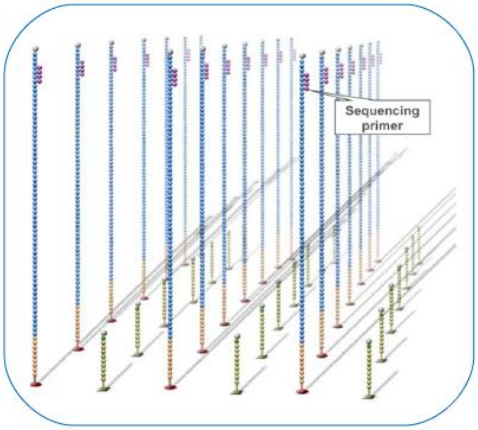

Figure 8. Annealing of sequencing primers

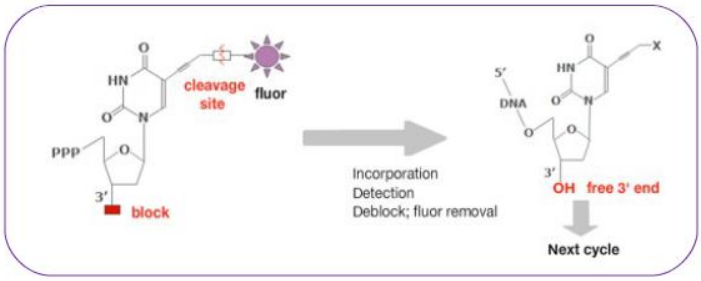

Figure 9. Chemical reaction on reversible terminators

Sequence analysis

The sequencing data obtained from MiSeq can be analyzed using dedicated software on the instrument computer using MiSeq Reporter or on a network server using BaseSpace 16S Metagenomics App (Illumina). Taxonomic Operational Units (OTUs) have been ranked taxonomically with an accurate GreenGenes database and computer data analysis has been carried out using the QIIME 1.8 "Quantitative Insights Into Microbial Ecology" program. To obtain more comparisons between the different samples, the ShannonWiener (H ') diversity index was calculated as:

$$H' = - \Sigma\, p_i \log_2 p_i$$

p_i= frequency of the i-th estimated taxon as n_i/N
N= the total number of individuals in the sample
n_i= abundance of the i-th sample taxon

This index takes into account the total number of OTUs (Operationale Taxonomic Units) and their relative prevalence within each sample.

CARAMEL STUDY - RESULTS

Characteristics of patients

From January 2013 to January 2016, 120 patients were assessed. Of these, 81/120 (67.5%) were male and 39/120 (32.5%) were females. The middle ages of patients was 62.2 years, with a range of ages 26 to 88 years.
All patients who had undergone at least one treatment cycle were evaluated with Ipilimumab. 100% of patients were found to be evaluable.
Patients exhibited primitive tumor at different sites. In particular: 50/120 (41.6%) had the primitive at the back / trunk level, 25/120 (20.8%) melanoma of upper or lower limbs, 20/120 (16.6%) acral melanoma, 11/120 (9.2%) uveal melanoma, 4/120 (3.3%) mucosal melanoma (rectal mucosa, oral cavity, oropharyngeal), 1 patient (0.8%) had retinal melanoma. Of 8/120 (6.7%) patients were unknown the home of the primitive.
100% of enrolled patients had metastatic disease: in particular 25/120 (20.8%) had M1a, 33/120 (27.5%) M1b, 59/120 (49.2%) M1c. Of 3/120 (2.5%) patients do not have the data on the sites of illness metastatic.
As for the ECOG-PS, most patients enrolled in the analysis had an excellent performance status at the start of treatment: 79/120 (65.8%) ECOGPS 0, 29/120 (24.2%) ECOG-PS 1, 10/120 (8.3%) ECOG-PS 2, 2/120 (1.7%) ECOG-PS 3. No patient had ECOG-PS 4.
69/120 (57.5%) patients were BRAF wild type, in 43/120 (35.8%) patients it was BRAF V600 mutation was found, while 8/120 (6.7%) patients were not mutational data is available. In all patients BRAF's mutational state was determined on the last surgically removed metastatic lesion.
Patients received the drug in different treatment lines: 57/120 (47.5%) line treatment for metastatic disease, 48/120 (40%) II line treatment, 15/120 (12.5%) treatment in III line.
The characteristics of the 120 patients enrolled are shown in the table below.

Clinical Features of patient enrolled	N (%)
Median Age (range)	(26-88)
SEX	
Male	81 (67,5)
Female	39 (32,5)
Primitive Tumor Site	
Back/trunk	50 (41,6)
Upper/lower limbs	25 (20,8)
Acral	20 (16,6)
Uveal	11 (9,2)
Mucosal	4 (3,3)
Retinal	1 (0,8)
Unknown	8 (6,7)

BRAF STATUS	
Wild Type	69 (57,5)
V600 Mutated	43 (35,8)
Unknown	8 (6,7)
ECOG PS	
0	79 (65,8)
1	29 (24,2)
2	10 (8,3)
3	2 (1,7)
Metastatic sites	
M1a	25 (20,8)
M1b	33 (27,5)
M1c	59 (49,2)
Unknown	3 (2,5)
IPI line of treatment	
First line	57 (47,5)
Second line	48 (40)
Third line	15 (12,5)

Survival analysis

In the 120 patients, a median survival of 17 months was observed (range 5-100 months).

Progression-free survival was 4.5 months (range 2-50 months).

In January 2016, 58/120 (48.3%) patients were alive, 56/120 (46.7%) patients were deceased, while 6/120 (5%) patients were lost to follow-up.

In the subgroup analysis, although it is not methodologically correct, we evaluated OS and PFS only about the administration of immunotherapy, ie the time between the beginning of immunotherapy (regardless of the previous lines) and the assessed progression or death or patient loss at follow up (this is the main reason why median OS and PFS are so different).

Prognostic value of clinical and laboratory parameters in terms of OS and PFS

Clinical parameters

As for the comparison of the survival curves by sex, males had an OS of 40 months vs. 17 months reported by the female subgroup (HR 0.28, p = 0.002, 95% CI 0.2442-0.7397). PFS was 21 months for male vs. 5 months for female population (HR 0.34, p = 0.003, 95% CI: 2,385-7,396).

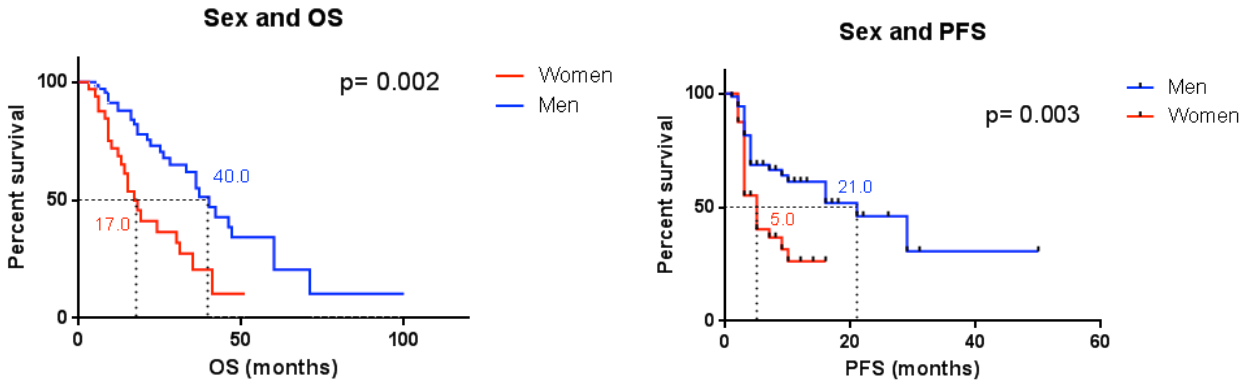

The presence of more than 3 sites of metastatic disease seems to be related to one worse OS and PFS. Patients with more than 3 disease sites had a 30-month OS compared to a 36-month OS of patients with less than 3 disease sites (HR 0.53, p <0.04, 95% CI: 0.6811-2.114).
For PFS, this was 5 months in patients with more than three sites metastatic disease vs 16 months of patients with less than 3 disease sites (HR 0.48 p < 0.03, 95% CI: 1.809-5.660).

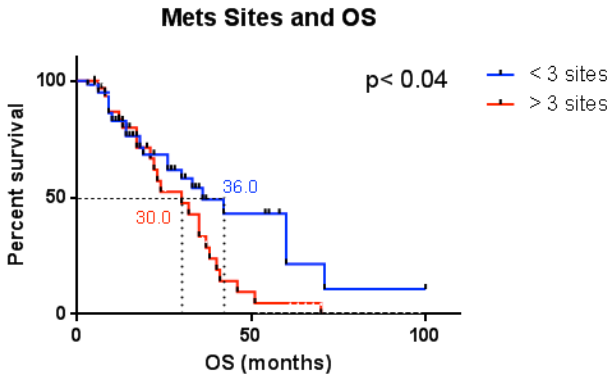

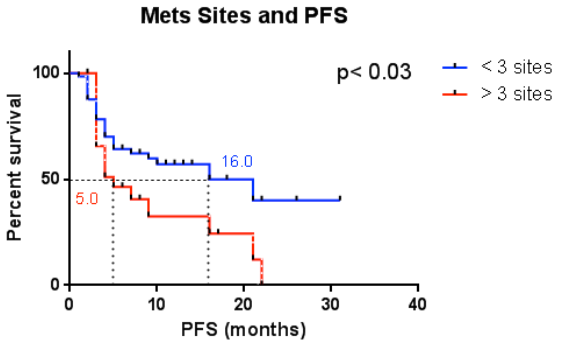

Survival was also evaluated in correlation with BRAF status. THE BRAF wild type patients presented a 33-month OS, while patients with BRAF mutation of a 30-month OS. This difference is not statistically significant significant (HR 0.90, p = 0.68, 95% CI 0.6085-1.989).
Also in terms of PFS, the comparison between BRAF wild type and BRAF-mutated population did not present statistically significant differences: both populations they presented a 16-month PFS (HR 0.97, p = 0.88, 95% CI 0.5508-1.816).

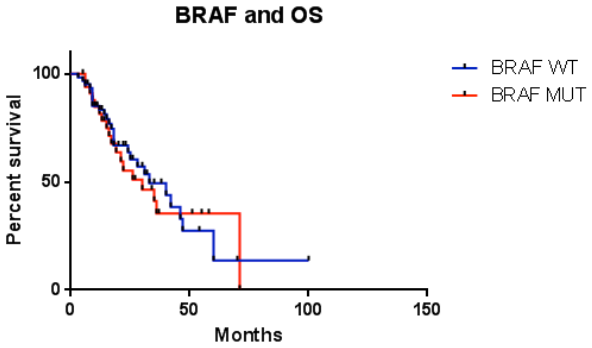

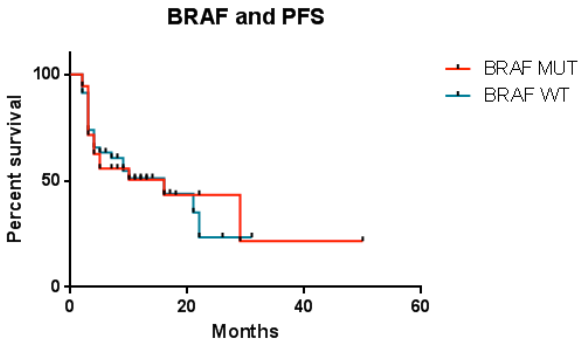

Patients were assessed on the basis of age, lower or greater than 65 years. The patients with less than 65 years of age had a 35-month OS compared to the 19 months of the patients with more than 65 years (HR 0.49, p <0.03, 95% CI 1.067-3.181). Instead, the PFS in patients under 65 years of age was 21 months vs. 12 months of older patients, although the difference was not statistically significant (HR 0.55, p = 0.93, 95% CI 0.9685-3.166).

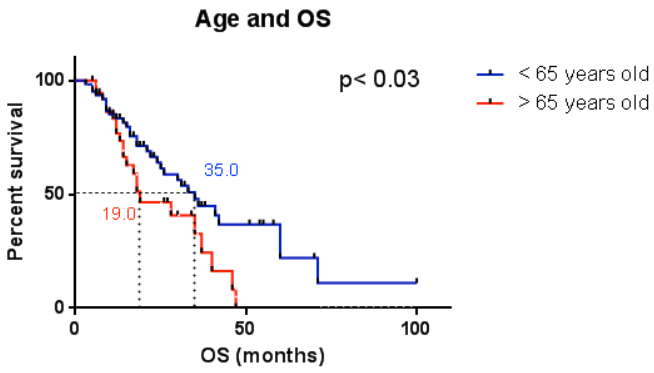

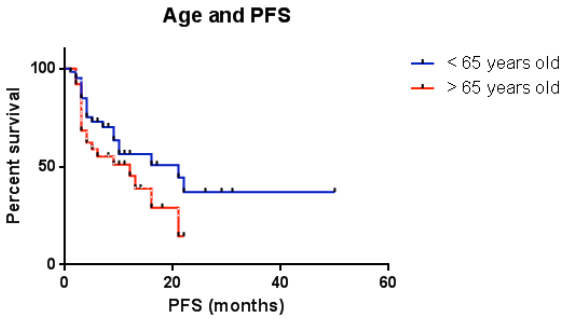

Laboratory parameters

The neutrophil count at baseline was evaluated in terms of OS and PFS. How long concerns the OS, patients with absolute neutrophils lower than cut-offs (cut-offs = 2003 / mmc) was 68 months versus 26 months of patients with an absolute number of neutrophils higher than cut-offs (HR 0.48, p = 0.03 95% CI 1,216-5,627). There PFS of patients with neutrophil count lower than cut-off was 29 months compared to 16 months of patients with lower neutrophil counts: this figure did not occur statistically significant (HR 0.59, p = 0.34, 95% CI 0.7604-4.321).

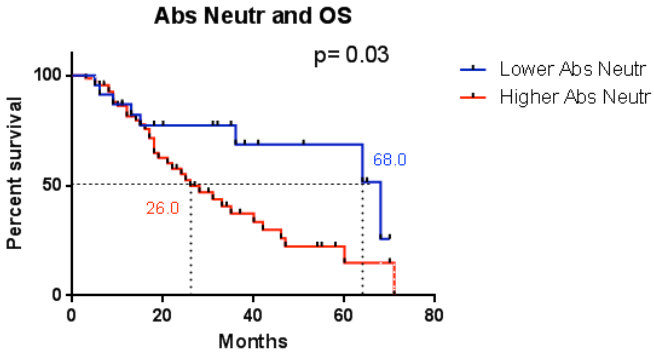

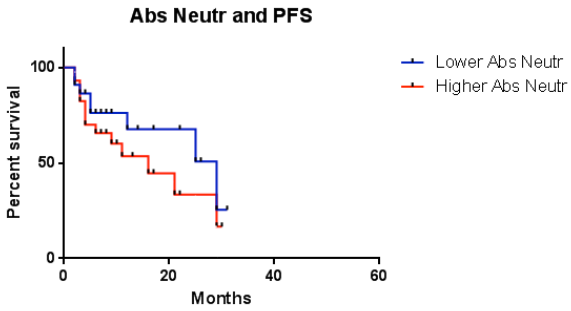

Patients with a lymphocyte count greater than cut-off (cut-off 1655 / mmc) have presented a 41-month OS vs. 24 months of patients with lower lymphatic counts (HR 0.52, p <0.04, 95% CI 0.9270-3.148). The PFS was 29 months for the patients with lymphocyte counts below cut-off compared to 4 months of patients with higher lymphocyte count (HR 0.33, p = 0.001, 95% CI 3.952-13.30).

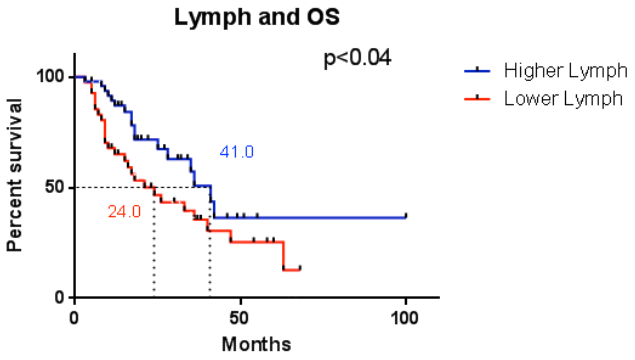

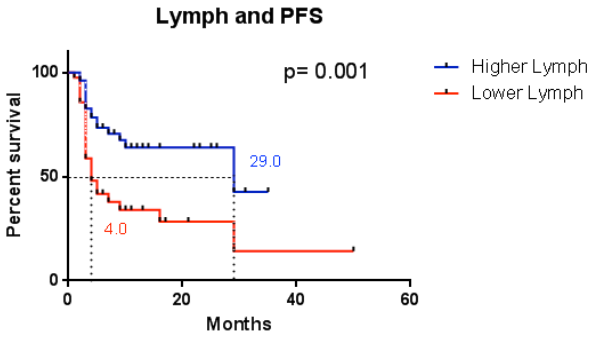

The eosinophil count evaluated at the baseline was not correlated either with the OS or with the PFS: patients with absolute eosinophil lower than cut-off (cut-off = 200 / mmc) have presented OS of 21 months compared to 26 months of patients with eosinophil counts higher than cut-off (HR 0.95, p = 0.92, 95% CI 0.3031-2.152); the PFS, instead, it was 17 months in patients with eosinophil counts lower than the cut-off vs. 22 months of eosinophilic patients higher than cut-off (HR 1.63, p = 0.28, 95% CI 0.3345-1.785).

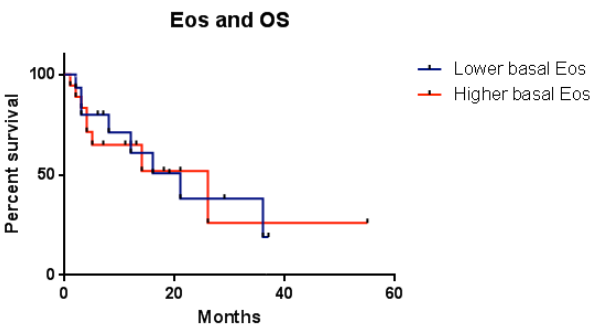

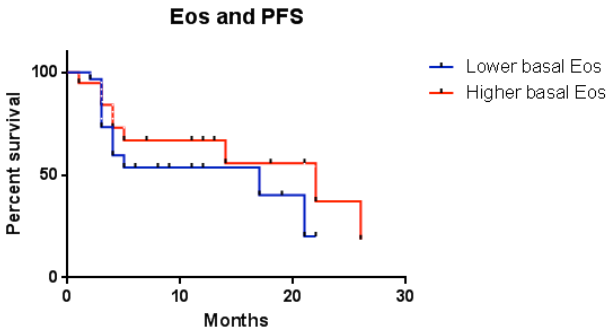

Regarding platelet count at baseline, patients with lower cut-offs (cut-off = 250000 / mcL) presented a 36-month OS vs. 26 months of patients with values above the cut-off: this result is not statistically significant (HR 0.86, p = 0.63, 95% CI 0.7690-2.493). Instead, PFS counts platelet lower than cut-off was 36 months vs. 25 months for patients with values higher (HR 0.48, p = 0.05, 95% CI 0.7725-2.684).

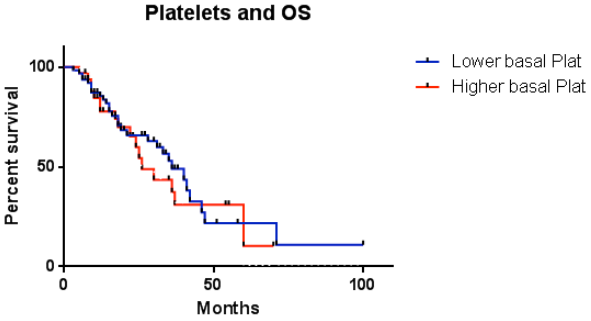

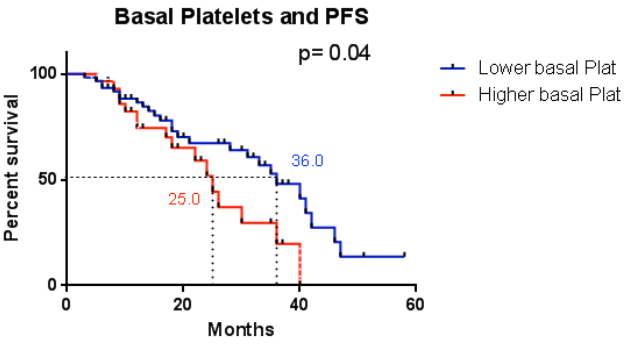

Overall survival of patients evaluated by LDH levels was found significantly different: in patients with high LDH values at the beginning of treatment (cut-off value 330 U / ml), a 26-month median OS was observed compared with 54 months of OS patients with lower LDH values than cut-offs. This difference is statistically significant (HR 0.49, p <0.05, 95% CI: 0.9124, -3.198).
This difference was also significant when the analysis was conducted relative to progression - free survival: in patients with serum LDH above the cut-off, a PFS of 4 months vs. 24 months was observed in patients with low LDH values. This difference was statistically significant (HR 0.34, p <0.01, 95% IC 3.284-10.96).

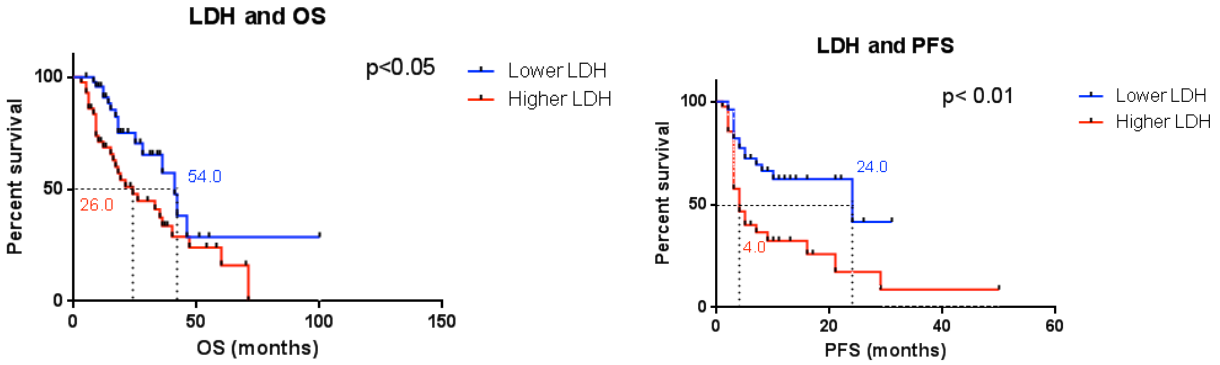

Regarding the role of the neutrophil / lymphocyte ratio (NLR, neutrophil-to-lymphocyte ratio), the analysis showed a detrimental effect of the high value of the baseline parameter, statistically significant result. In particular, considering how cut-off the value of 2.5, patients with high NLR had a 26 - month OS compared to population with low NLR who presented a 35-month OS (HR 0.92, p <0.0001, 95% IC 0.7102-2.552).
The same data evaluated for the PFS showed that the population with NLR at above the cut-off had a 7-month PFS vs 26-month PFS of the subgroup with NLR below the cut-off. However, this result is not statistically significant (HR 0.65, p = 0.35, 95% IC 2.035-6.781).

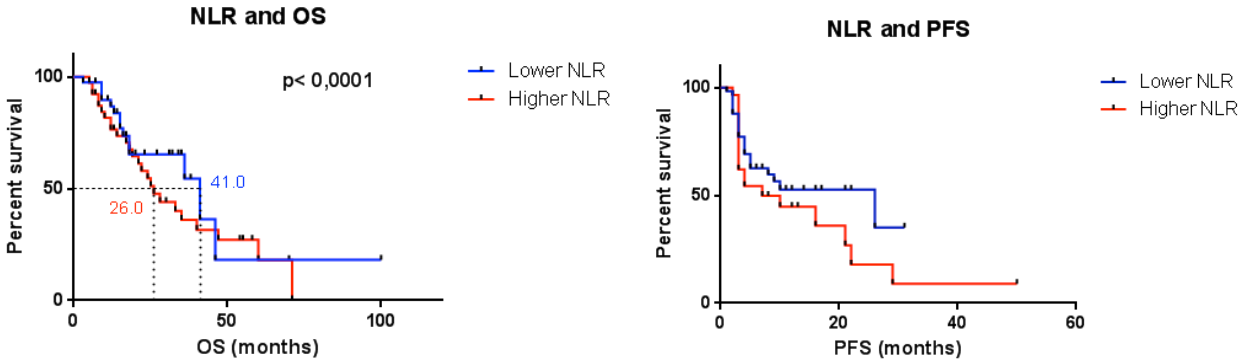

As far as platelet / lymphocyte ratio (PLR) is concerned, considering how cut-off the value of 121, we saw that patients with PRL at below the cut-off value they had an OS of 54 months compared

to the OS of 26 months of patients with PLR above the cut-off value (HR 0.51, p <0.05, 95% IC 0.9593-4.496).

By evaluating the parameter in terms of progression free survival, patients with Low PRL presented a 27-month PFS vs 7-month PFS in patients with PLR high (HR 0.47, p = 0.02, 95% IC 1.886-7.890).

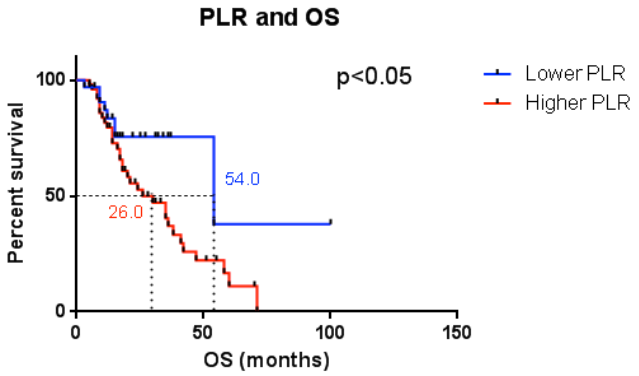

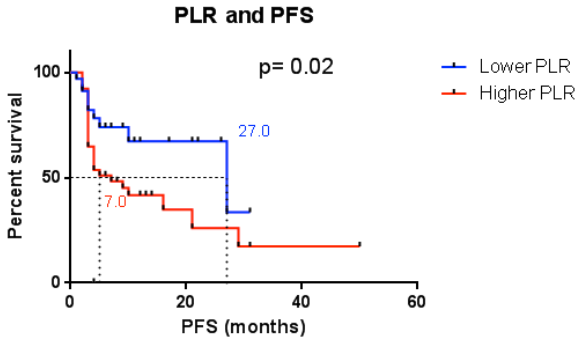

We evaluated the neutrophil / eosinophil ratio (NER, neutrophil-to-eosinophil ratio) with survival. Patients with NER below cut-off (cut-off: 26.10) have presented a 51-month vs. 25-month OS of patients with NER above the cut-off (p = 0.31, 95% IC 0.8051-5.169 HR 0.72). As for the progression free from disease, the group of patients with low NER presented one PFS of 12 months vs. 4 months of patients with NER high (HR 0.60, p 0.33, 95% IC 1.163- 7,739). However, both values did not show statistically significant.

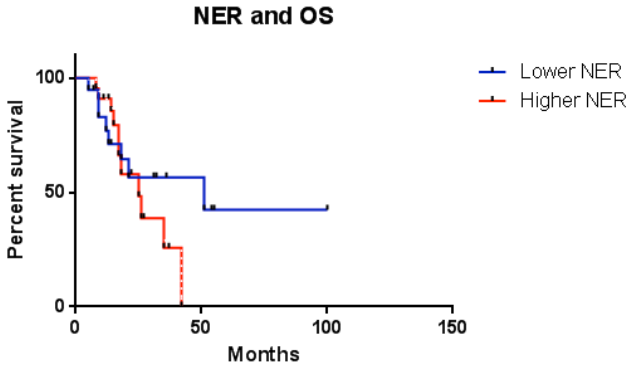

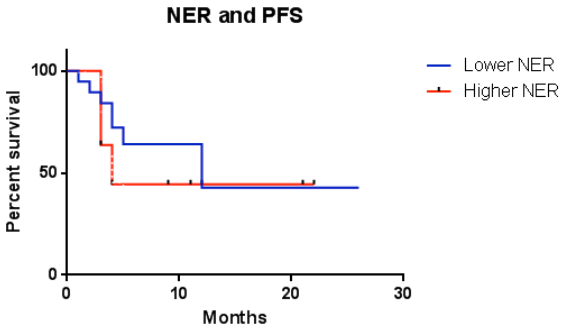

As far as the platelet / eosinophil ratio is concerned, patients with a lower ratio of cut-off (cut-off = 1477) showed a 34-month OS compared to the 25 months of the cut-off patients with a higher cut-off ratio (HR 0.74, p = 0.56, 95% CI 0.5247-3.525), not statistically significant. The PFS of Relative Patients lower than cut-off was 12 months versus 4 months of patients with higher than cut-off (HR 0.71, p = 0.12, 95% CI 0.3039-1.695), even in this case statistically significant.

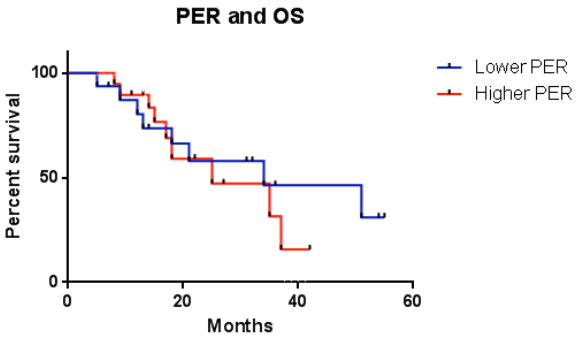

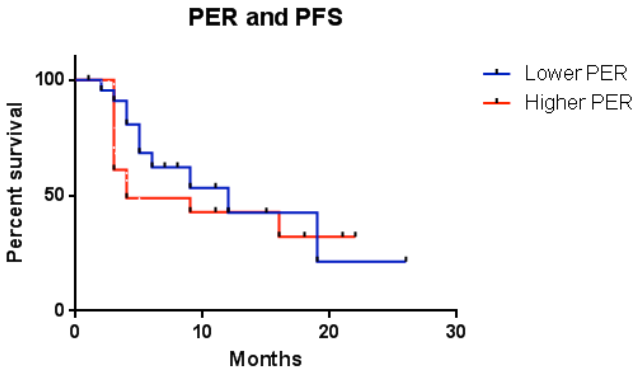

Correlation analysis between clinical and laboratory parameters and OS and PFS data

When evaluating the absolute values of the laboratory parameters, a correlation statistically significant was found between the PFS and the basal absolute value of neutrophils (r = -374, p <0.001), lymphocytes (r = 0.217, p = 0.042), baseline platelet counts (r = -238, p = 0.022), the LDH value (r = -0.202, p = 0.045), the ratio neutrophils / eosinophiles (r = -0.305, p = 0.044) and the platelet / eosinophil ratio (r = -0.320, p = 0.036).

As for the OS, a significant correlation was found to be the value of neutrophils (r = -0.303, p = 0.004) and neutrophil / eosinophilic ratio (r = -0.301, p = 0.038).

In addition, the OS correlated significantly with sex, that is, the male has had a greater female survival (r = -0.215, p = 0.028) and with age, in the sense that under 65 years of age was associated with greater survival (r = - 0.205, p = 0.042).

In the multivariate correlation analysis, the baseline value of LDH (coefficient beta = - 0.322, p = 0.043) (figure 19) and platelets (coefficient beta -2.129, p = 0.040) have been shown to be independent predictors of PFS; while the value of neutrophils was the predictor of OS (coefficient beta = -0.335, p = 0.026).

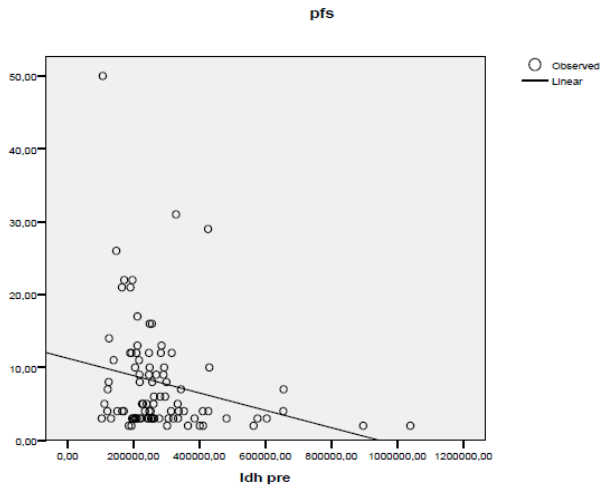

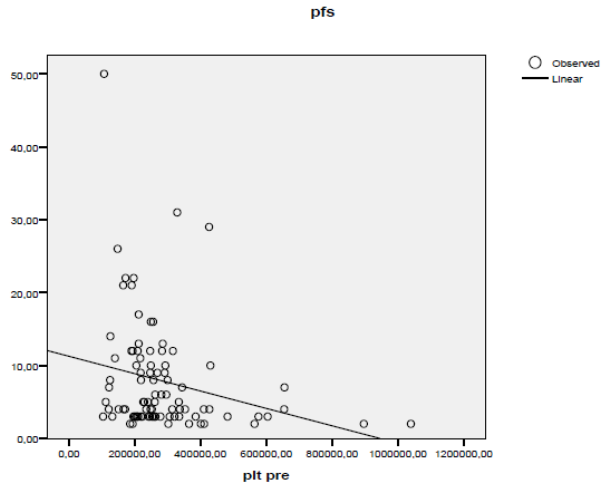

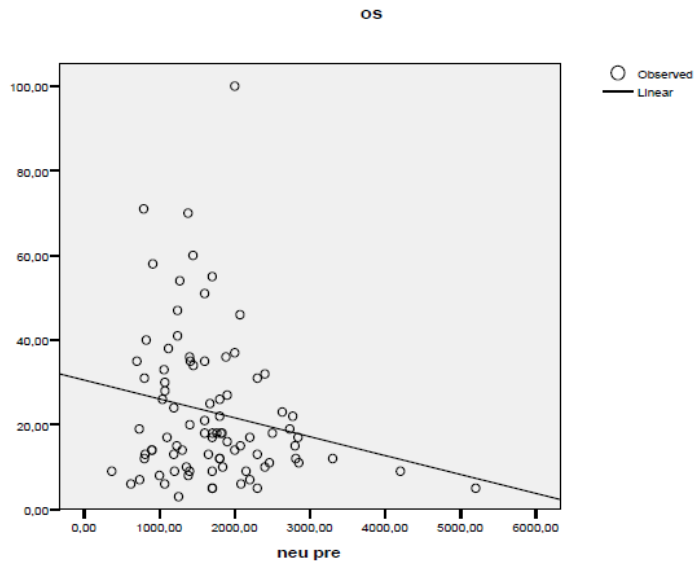

In conclusion, we'd like to underline that all markers taken into account for the assessment of the impact on PFS and OS are not expected to be *a priori* used for selecting responder or resistant patients. Surely a very positive aspect of the work is that the patients' population came from the real life and, if from one side this may represent an additional value, on the other one the series of analyzed patients is too heterogeneous to be grouped and there is a need for much higher number of cases in order to appropriately evaluate the different subgroups of patients (i.e. the eterogeneity is also increased by the different schedules of treatment, number of treatment administration, previous therapies and so on).

CREAM STUDY – RESULTS

The CREAM study turns out to be the first study conducted on immunotherapy patients which evaluates the intestinal microbiote and the possible relationship between the clinical outcome and the dysbiosis that these patients often present. We could consider it as a pilot study, in terms of reduced number of patients enrolled (25 patients, even if most of them not evaluable because of the discontinuation of treatment due to different causes), in which we collected a sample of faecal material before the beginning of therapy and every 3 or 4 cycles (depending on Nivolumab every 2 weeks or Pembrolizumab every 3 weeks), for at least three following measurements.
In the figures below we report the results of the patient-divided sampling, in which the different intestinal bacteria were isolated, identifying for each of them the phylum, the family and the genus.
In particular about the genus, we identified an alteration of the Akkermansia Muciniphila in 4 patients enrolled, the only patients who developed a colitis with grade II-III diarrhea, which required a temporary suspension of treatment and the setting of a correct steroid therapy.

PHYLUM

ID	Firmicutes	Bacteroidetes	Proteobacteria	Actinobacteria	Cyyanobacteria	Verrucomicrobia	Chloroflexi

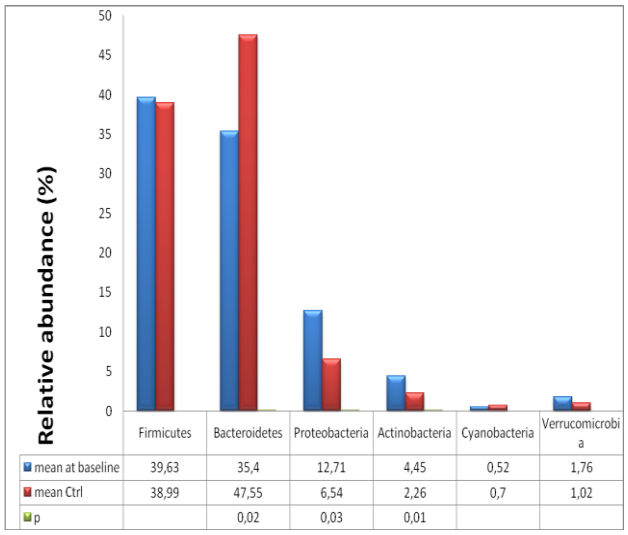

	Firmicutes	Bacteroidetes	Proteobacteria	Actinobacteria	Cyanobacteria	Verrucomicrobia
mean at baseline	39,63	35,4	12,71	4,45	0,52	1,76
mean Ctrl	38,99	47,55	6,54	2,26	0,7	1,02
p		0,02	0,03	0,01		

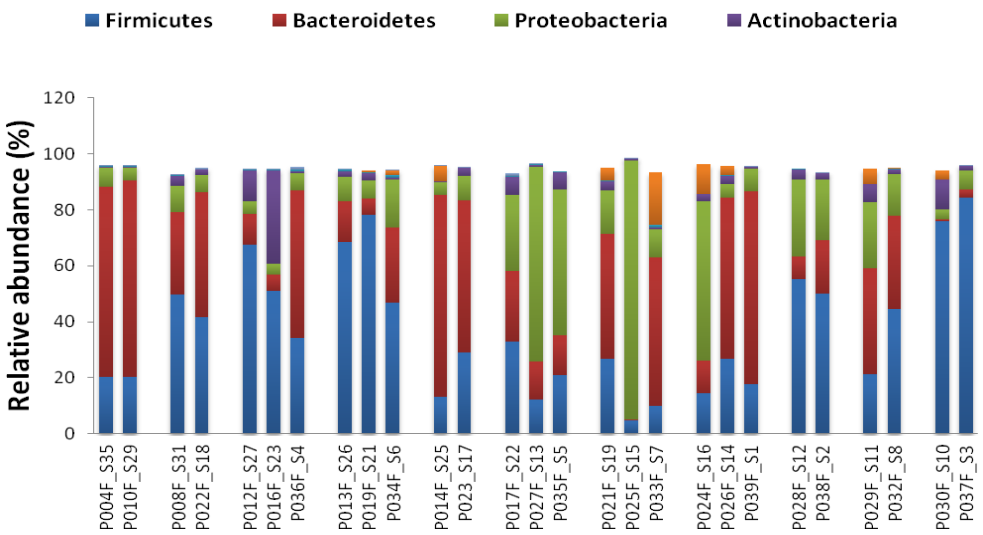

P004F_S35	20,43	67,77	6,75	0,32	0,52	0	0,31
P010F_S29	20,17	70,38	4,53	0,22	0,46	0	0,34
P008F_S31	49,61	29,68	9,44	3,47	0,25	0	0,36
P022F_S18	41,59	44,8	6,1	1,81	0,26	0	0,42
P012F_S27	67,59	10,82	4,82	10,76	0,28	0	0,44
P016F_S23	51,17	5,78	3,74	33,43	0,19	0	0,2
P036F_S4	34,14	52,91	6,2	0,58	0,66	0	0,87
P013F_S26	68,37	14,62	8,7	1,98	0,6	0	0,12
P019F_S21	78,2	5,78	6,66	2,47	0,2	0,69	0
P034F_S6	46,81	26,76	17,22	0,72	0,85	1,65	0,28
P014F_S25	13,23	72,08	4,58	0,36	0	5,37	0,22
P023_S17	29,09	54,25	8,84	2,83	0	0	0,25
P017F_S22	33,01	25,08	27,12	6,48	0,58	0	0,83
P027F_S13	12,26	13,63	69,5	0,53	0,33	0	0,24
P035F_S5	21,07	14,07	52,1	6,36	0,26	0	0
P021F_S19	26,66	44,79	15,61	3,06	0,54	4,42	0
P025F_S15	4,61	0,48	92,49	0,68	0,08	0,02	0,02
P033F_S7	9,98	53,09	10,06	0,72	0,86	18,84	0
P024F_S16	14,35	11,72	56,99	2,59	0,09	10,66	0
P026F_S14	26,85	57,54	4,92	2,87	0,16	3,33	0
P039F_S1	17,6	69,16	7,9	0,63	0,12	0	0,35
P028F_S12	55,37	7,87	27,71	3,37	0,17	0	0
P038F_S2	49,94	19,25	21,59	2,23	0,08	0	0,1
P029F_S11	21,26	37,94	23,52	6,47	0,1	5,29	0
P032F_S8	44,54	33,24	15,06	1,71	0,29	0,05	0
P030F_S10	75,91	0,83	3,38	10,88	0	3,17	0
P037F_S3	84,35	2,81	6,96	1,64	0,09	0	0,14

FAMILY

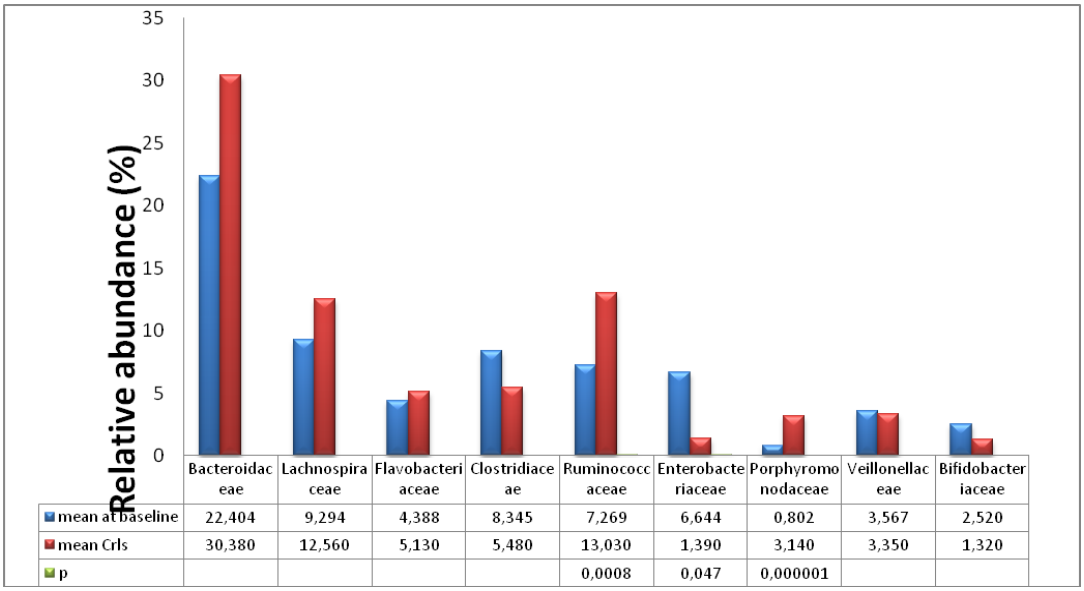

	Bacteroidaceae	Lachnospiraceae	Flavobacteriaceae	Clostridiaceae	Ruminococcaceae	Enterobacteriaceae	Porphyromonadaceae	Veillonellaceae	Bifidobacteriaceae
mean at baseline	22,404	9,294	4,388	8,345	7,269	6,644	0,802	3,567	2,520
mean Crls	30,380	12,560	5,130	5,480	13,030	1,390	3,140	3,350	1,320
p					0,0008	0,047	0,000001		

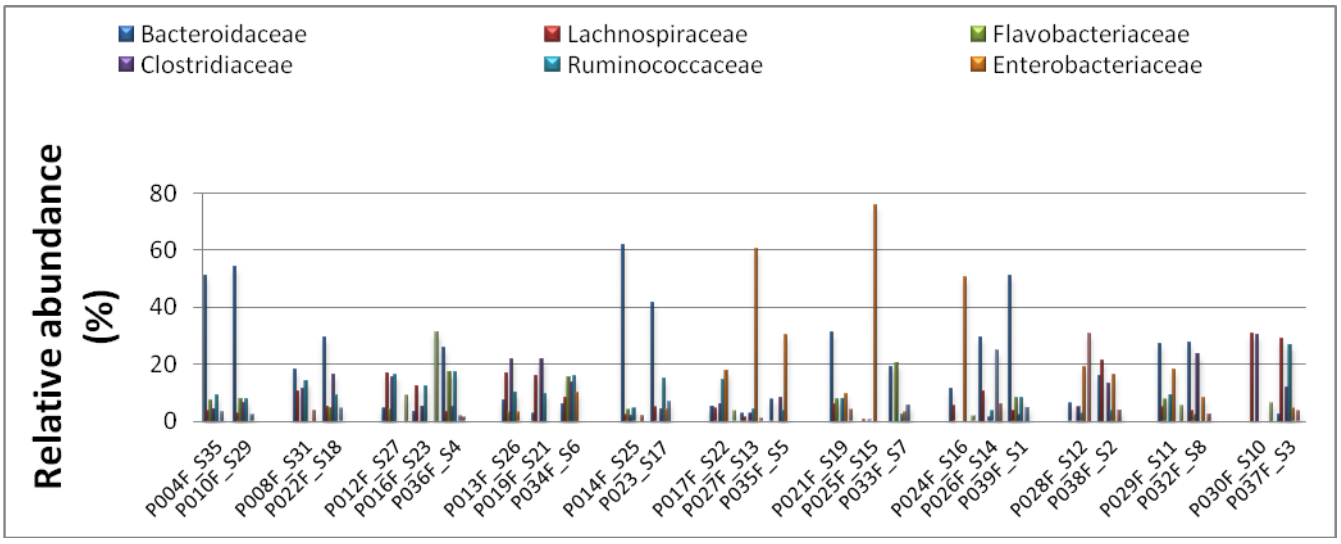

ID	Bacter	Lachnospir	Flavobact	Clostr	Ruminoc	Enterobact	Porphyr	Veillonel	Bifidobac

P004F_S35	51,06	3,49	7,37	4,19	9,2	0	3,29	0	0
P010F_S29	54,3	2,65	7,73	6,31	7,87	0	2,19	0	0
P008F_S31	18,21	10,37	0	11,4	13,87	0	0	3,85	0
P022F_S18	29,4	4,99	4,67	16,19	8,85	0	4,48	0	0
P012F_S27	4,45	16,76	4,25	15,42	16,09	0	0	0	9,04
P016F_S23	3,38	12,06	0	5,15	12,42	0	0	0	30,95
P036F_S4	25,85	3,41	17,29	4,99	17,1	0	1,78	1,53	0
P013F_S26	7,31	16,65	3,11	21,45	9,97	2,98	0	0	0
P019F_S21	2,83	15,65	0	21,52	9,67	0	0	0	0
P034F_S6	5,92	8,08	15,41	13,41	15,72	9,89	0	0	0
P014F_S25	61,75	2,27	4,11	2,03	4,41	0	0	2,02	0
P023_S17	41,56	4,89	0	4,22	14,74	4,21	6,69	0	0
P017F_S22	5,1	4,53	0	6,04	14,66	17,79	0	0	3,44
P027F_S13	2,68	1,4	0	2,83	4,21	60,55	0	0,99	0
P035F_S5	7,5	0	0	8,26	3,85	30,29	0	0	0
P021F_S19	31,08	6,03	7,71	0	7,91	9,32	0	3,9	0
P025F_S15	0	0,56	0	0,39	0	75,8	0	0	0
P033F_S7	19,17	0	20,49	0	2,51	3,08	5,51	0	0
P024F_S16	11,25	5,28	0	0	0	50,29	0	0	1,84
P026F_S14	29,45	10,45	0	1,38	3,5	0	25,02	5,99	0
P039F_S1	50,78	3,58	8,37	2,39	8,21	0	4,69	0	0
P028F_S12	6,19	0	0	4,78	2,62	19,07	0	30,7	0
P038F_S2	15,97	21,43	0	13,27	3,52	16,06	0	3,82	0
P029F_S11	27,03	4,88	7,51	0	8,87	18,23	0	0	5,49
P032F_S8	27,43	3,6	2,39	23,27	0	7,96	0	2,49	0
P030F_S10	0	30,64	0	30,03	0	0	0	0	6,39
P037F_S3	2,5	28,69	0	11,6	26,8	4,34	0	3,45	0

GENUS

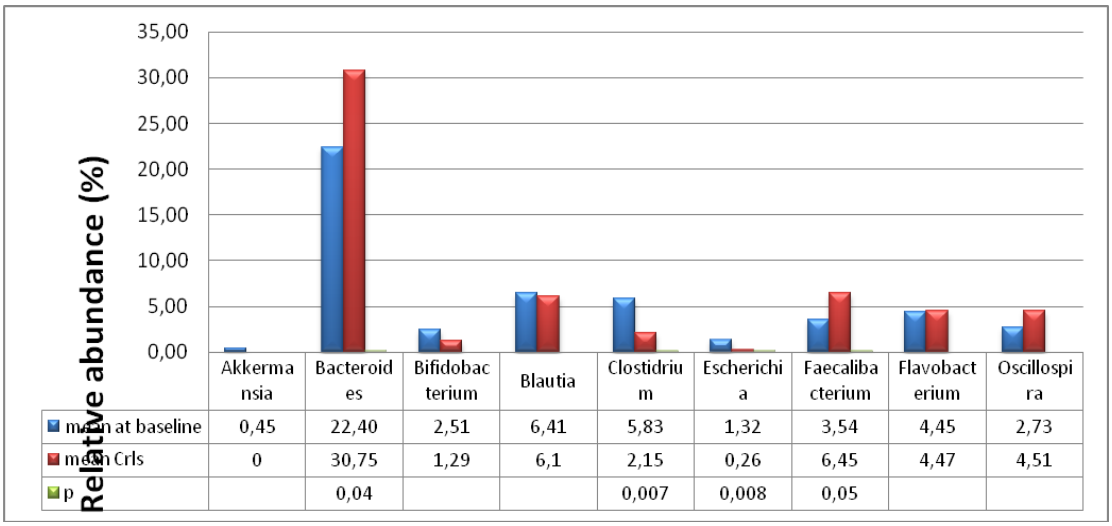

	Akkermansia	Bacteroides	Bifidobacterium	Blautia	Clostidrium	Escherichia	Faecalibacterium	Flavobacterium	Oscillospira
mean at baseline	0,45	22,40	2,51	6,41	5,83	1,32	3,54	4,45	2,73
mean Crls	0	30,75	1,29	6,1	2,15	0,26	6,45	4,47	4,51
p		0,04			0,007	0,008	0,05		

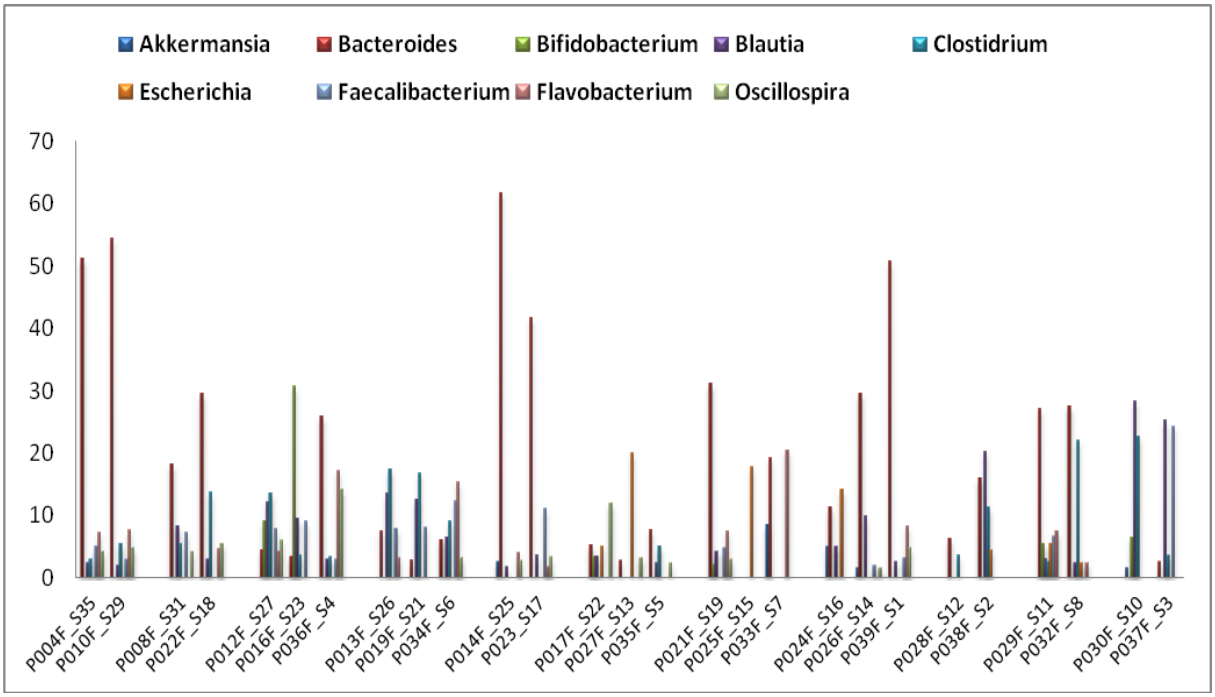

ID	Akkerm	Bacteroid	Bifidobacter	Blautia	Clostidr	Escheric	Faecalibact	Flavobact	Oscillosp
P004F_S35	0	51,06	0	2,37	2,97	0	4,91	7,19	4,12

P010F_S29	0	54,3	0	1,86	5,32	0	2,92	7,55	4,7
P008F_S31	0	18,21	0	8,27	5,32	0	7,14	0	4,1
P022F_S18	0	29,4	0	2,91	13,76	0	0	4,55	5,47
P012F_S27	0	4,45	8,96	11,99	13,48	0	7,9	4,21	6,05
P016F_S23	0	3,38	30,69	9,38	3,59	0	8,94	0	0
P036F_S4	0	25,85	0	2,91	3,29	0	2,97	17,12	14,08
P013F_S26	0	7,31	0	13,48	17,29	0	7,74	3,06	0
P019F_S21	0	2,83	0	12,45	16,68	0	7,98	0	0
P034F_S6	0	5,92	0	6,39	8,95	0	12,2	15,29	3,16
P014F_S25	2,54	61,75	0	1,73	0	0	0	4,01	2,73
P023_S17	0	41,56	0	3,59	0	0	11	1,81	3,26
P017F_S22	0	5,1	3,41	3,43	0	4,92	0	0	11,94
P027F_S13	0	2,68	0	0	0	19,92	0	0	3,18
P035F_S5	0	7,5	0	2,27	5,05	0	0	0	2,27
P021F_S19	0	31,08	2,16	4,08	0	0	4,68	7,3	2,9
P025F_S15	0	0	0	0	0	17,7	0	0	0
P033F_S7	8,44	19,17	0	0	0	0	0	20,32	0
P024F_S16	4,87	11,25	0	4,88	0	14,03	0	0	0
P026F_S14	1,46	29,45	0	9,77	0	0	1,93	0	1,56
P039F_S1	0	50,78	0	2,54	0	0	3,14	8,23	4,84
P028F_S12	0	6,19	0	0	3,6	0	0	0	0
P038F_S2	0	15,97	0	20,16	11,22	4,38	0	0	0
P029F_S11	0	27,03	5,44	3,04	2,59	5,38	6,63	7,38	0
P032F_S8	0	27,43	0	2,3	21,95	2,28	0	2,34	0
P030F_S10	1,45	0	6,35	28,21	22,54	0	0	0	0
P037F_S3	0	2,5	0	25,31	3,52	0	24,21	0	0

From these preliminary and reduced data, it is certainly difficult to understand precisely what role the representation of Akkermansia can have in the pathogenesis of colitis by immunotherapy,

although recently the study by York A. showed how it can play a key role in both regulation of homeostasis of intestinal bacterial flora in the development of colitis.
It would be auspicable to continue the study with a higher enrollment of patients and the collection of serial faecal samples up to 6-12 months from the beginning of the therapy, in order to evaluate if this alteration is able to maintain itself over time or, eventually, alter further the balance of intestinal flora.

COFFEE STUDY – RESULTS

Overall survival based on LDH levels was found significantly different: in patients with high LDH values at the beginning of treatment (cut-off value 245 U/ml), a 13-month median OS was observed compared with 44 months of OS patients with lower LDH values than cut-offs. This difference is statistically significant (HR 0.25, p =0.02, 95% CI: 1.227 – 9.334).
This difference was also significant when the analysis was conducted for progression - free survival: in patients with serum LDH above the cut-off, a PFS of 5 months vs. 29 months was observed in patients with low LDH values.
This difference was statistically significant (HR 0.22, p =0.01, 95% IC 2.103-15.99).

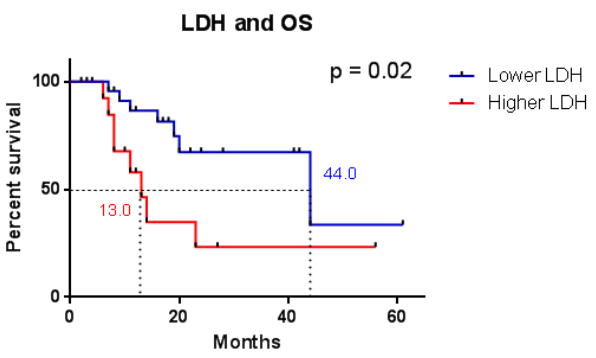

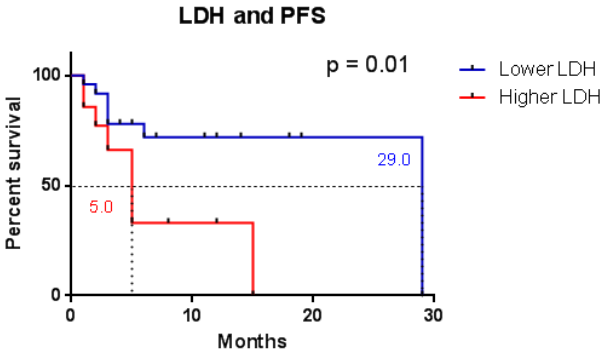

The comparison of the survival curves by sex shows that males had an OS of 23 months vs. 44 months reported by the female subgroup (HR 0.51, p = 0.8, 95% CI 0.1622-1.649). PFS was 15 months for male vs. 29 months for female population (HR 0.52, p = 0.003, 95% CI: 0.1610-1.697).

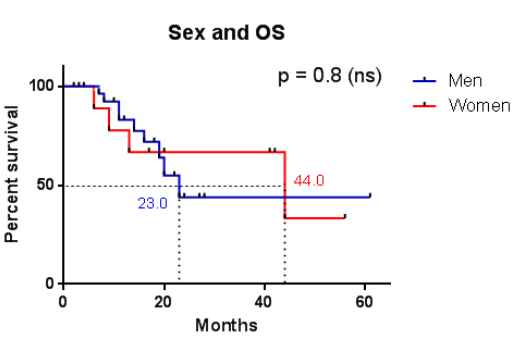

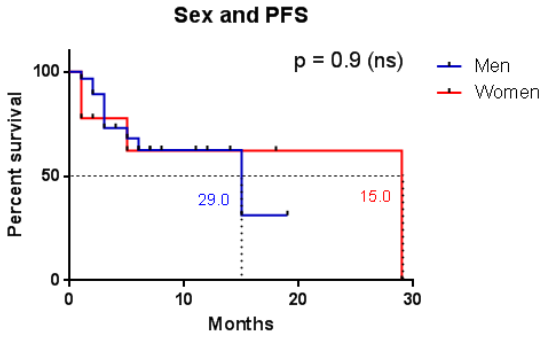

The presence of more than 3 sites of metastatic disease is related to one worse OS and PFS. Patients with more than 3 mets sites had a 14-month OS compared to a 44-month OS of patients with less than 3 disease sites (HR 0.31, p =0.01, 95% CI: 0.1154-0.8774).
PFS was 5 months in patients with more than three sites metastatic disease vs 29 months of patients with less than 3 disease sites (HR 0.14 p = 0.005, 95% CI: 2.103-15.99).

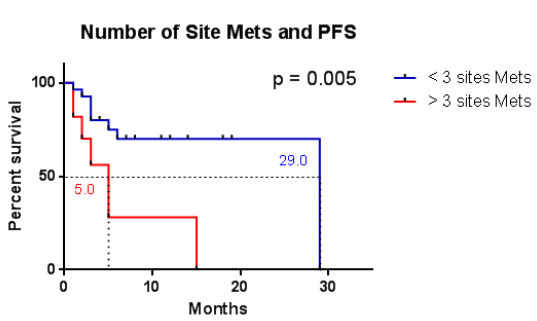

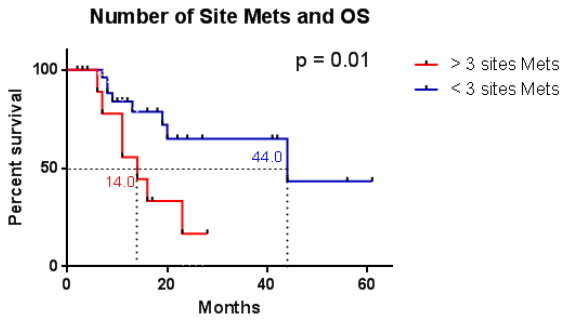

Patients were assessed also on the basis of age, lower or greater than 70 years. The patients with less than 70 years of age had a 23-month OS compared to the 44 months of the patients with more than 70 years (HR 1.07, p =0.5, 95% CI 0.1876-1.426). Instead, the PFS in patients under 70 years of age was 15 months vs. 29 months of older patients, although the difference was not statistically significant in both cases (HR 1.37, p = 0.8, 95% CI 0.1896-1.442).

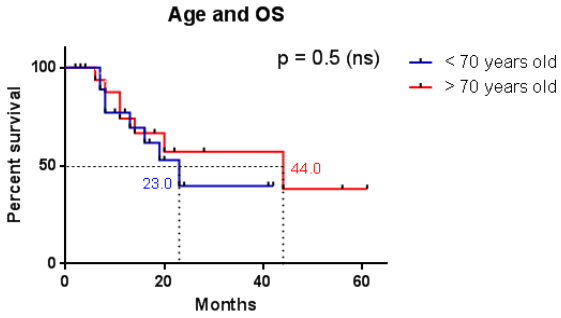

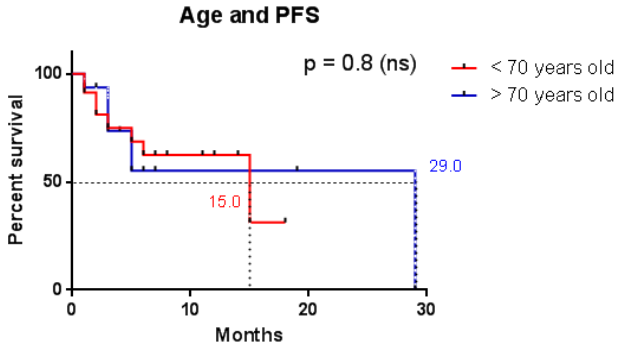

The most interesting issue of the research was the evaluation of PFS and OS in relation to the use of antibiotics within 30 days of the onset of immunotherapy treatment: patients who assumed antibiotics before therapy assessed a PFS of 3 months vs. 29 month of others (HR 9.54, p < 0.0001, 95% CI 0.0291-0.3666). Also OS was significantly higher for those who didn't assume any antibiotics before therapy, 44 months vs. 14 months (HR 5.03, p = 0.0019, 95% CI 0.1026-0.9866).

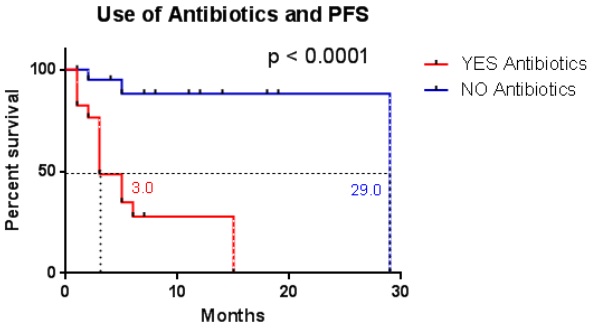

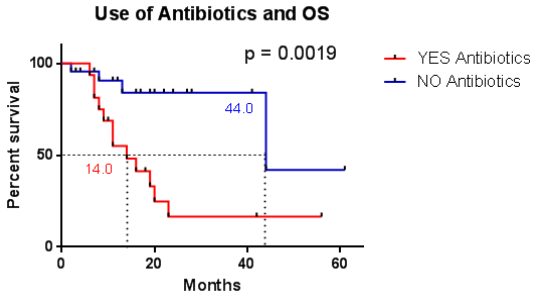

Regarding the COFFEE study, we performed an evaluation of the single laboratory parameters of the blood count (neutrophil counts, eosinophils, basophils, platelets and their ratio), which showed a statistical significance (data not shown) to the univariate analysis, although the multivariate analysis has not been performed.

The originality of this study is certainly the evaluation of these parameters with new generation immunotherapies (checkpoint inhibitors), since we are not aware that similar studies have been reported in the literature yet.

As in the CARAMEL study, also in this case the patients enrolled were a real life population, and this is definitely a strong point but, on the other hand, it represents a limit for sample inhomogeneity and patient stratification not performed in methodically correct way.

Beyond the single variables of the blood count and LDH, we found useful and interesting to explore other characteristics such as sex, the number of metastatic sites (greater or less than 3) and the possible interference of antibiotic therapy administered within 30 days prior to therapy: this last fact, in our opinion, represents the novelty of research in this field. The difference in terms of overall survival and progression free survival was so significant that antibiotic intake in the 30 days prior to the start of therapy seems to have a detrimental role in the efficacy of the therapy itself.

Naturally, these data should be confirmed and possibly correlated with a multivariate analysis, and also the patient sample should be numerically larger and more homogeneous from the clinical and pathological point of view (possibly enroll in the study patients in the first line treatment).

Bibliography

1. *Galon J, Angell HK, Bedognetti D, et al. The continuum of cancer immunosurveillance:prognostic, predictive, and mechanistic signatures. Immunity 2013;39(1):11-26*
2. *Oliveira Cobucci RN, Saconato H, Lima PH, et al. Comparative incidence of cancer in HIV-AIDS patients e transplant recipients. Cancer Epidemol 2012; 36(2): e69-73*
3. *Carmine Pinto. Immuno-Oncologia generale. Il pensiero Scientifico Editore 2015*
4. *Miller JF, Sadelain M. The journey from discoveries in fundamental immunology to cancer therapy. Cancer Cell 2015; 27(4); 439-49*
5. *Schalper KA, Brown J, Carvajal-Hausdorf D, et al. Objective measurement and clinical significance of TILs in non-small cell lung cancer. J Natl Canc Inst 2015; 107(3).*
6. *Galon J, Mlecnik B, Bindea G, et al. Towards the introduction of the 'Immunoscore' in the classification of malignant tumours. J Pathol 2014; 232(2); 199-209*
7. *Chen DS, Mellman I. oncology meets immunology: the cancer immunity cycle. Immunity 2013; 39(1): 1-10*
8. *Mittal D, Gubin MM, Schreiber RD, et al. New insights into cancer immunoediting and its three component phases – elimination, equilibrium and escape. Curr Opin Immunol 2014; 27:16-25*
9. *Adachi K, Tamada K. Immune checkpoint blockade opens an avenue of cancer immunotherapy with a potent clinical efficacy. Cancer Sci 2015; doi:10.1111/cas.12695*
10. *Vesely MD, Schreiber RD. Cancer immunoediting: antigens, mechanism, and implications to cancer immunotherapy. Ann N Y Acad Sci 2013; 1284:1-5*
11. *O'Day SJ, Hamid O, Urba WJ. Targeting cytotoxic T-lymphocyte antigen-4 (CTLA-4): a novel strategy for the treatment of melanoma and other malignancies. Cancer 2007; 110(12):2614-27*
12. *Sanderson K, Scotland R, Lee P, et al. Autoimmunity in a phase I trial of a fully human anti-cytotoxic T-lymphocyte antigen-4 monoclonal antibody with multiple melanoma peptides and Montanide ISA 51 for patients with resected stages III and IV melanoma. J Clin Oncol. 2005; 23:741– 750*
13. *Faries MB, Hsueh EC, Shu S, et al. Post-vaccination CTLA- 4 expression correlates inversely with survival in patients vaccinated with allogeneic melanoma cell vaccine. J Clin Oncol. 2004; 22(14S):2565*
14. *Pardoll DM. The blockade of immune checkpoints in cancer immunotherapy. Nat Rev Cancer 2012; 12(4):252–264*
15. *Eckburg PB et al. Diversity of the human intestinal microbial flora. Science. 2005 Jun 10;308(5728):1635-8*
16. *Raoult D. et al. Creationism--remember the principle of falsifiability. Lancet 2008 Dec 20;372(9656):2095-6*
17. *Koboziev I et al. Role of the enteric microbiota in intestinal homeostasis and inflammation. Free Radic Biol Med 2014 Mar;68:122-33.*

18. *Mariat D, Firmesse O, Levenez F, Guimarães V, Sokol H, Doré J, Corthier G, Furet JP. The Firmicutes/Bacteroidetes ratio of the human microbiota changes with age. BMC Microbiol. 2009 Jun 9;9:123*
19. *Zoetendal EG, Akkermans AD, De Vos WM Temperature gradient gel electrophoresis analysis of 16S rRNA from human fecal samples reveals stable and host-specific communities of active bacteria. Appl Environ Microbiol. 1998 Oct;64(10):3854-9*
20. *Ley RE, Peterson DA, Gordon JI. Ecological and evolutionary forces shaping microbial diversity in the human intestine. Cell. 2006 Feb 24;124(4):837-48*
21. *Milani C, Ferrario C, Turroni F, Duranti S, Mangifesta M, van Sinderen D, Ventura M. The human gut microbiota and its interactive connections to diet. J Hum Nutr Diet. 2016 Oct;29(5):539-46*
22. *Hayashi H, Sakamoto M, Benno Y. Fecal microbial diversity in a strict vegetarian as determined by molecular analysis and cultivation. Microbiol Immunol. 2002;46(12):819-31*
23. *Bäckhed F, Ley RE, Sonnenburg JL, Peterson DA, Gordon JI. Host-bacterial mutualism in the human intestine. Science. 2005 Mar 25;307(5717):1915-20*
24. *Turroni F, Ribbera A, Foroni E, van Sinderen D, Ventura M. Human gut microbiota and bifidobacteria: from composition to functionality. Antonie Van Leeuwenhoek. 2008 Jun;94(1):35-50*
25. *Wexler HM. Bacteroides: the good, the bad, and the nitty-gritty. Clin Microbiol Rev. 2007 Oct;20(4):593-621*
26. *Kharpa KD, Vrana KE. Creating a virtual pharmacology curriculum in a problem-based learning environment: one medical school's experience. Acad Med. 2013 Feb;88(2):198-205*
27. *Zhang T Breitbart M, Lee WH, Run JQ, Wei CL, Soh SW, Hibberd ML, Liu ET, Rohwer F, Ruan Y. RNA viral community in human feces: prevalence of plant pathogenic viruses. PLoS Biol. 2006 Jan;4(1):e3.*
28. *Lepage P, Seksik P, Sutren M, de la Cochetière MF, Jian R, Marteau P, Doré J. Biodiversity of the mucosa-associated microbiota is stable along the distal digestive tract in healthy individuals and patients with IBD. Inflamm Bowel Dis. 2005 May;11(5):473-80.*
29. *Riley PA, Melanoma and problem of malignancy. Tohoku J Exp Med. 2004 Sep;204(1):1-9*
30. *Newberry RD, Lorenz RG. Organizing a mucosal defense. Immunol Rev. 2005 Aug;206:6-21*
31. *Paula Peruzzi E et al., 2015*
32. *Sekirov I, Russell SL, Antunes LC, Finlay BB. Gut microbiota in health and disease. Physiol Rev. 2010 Jul;90(3):859-904*
33. *Mirpuri J, Raetz M, Sturge CR, Wilhelm CL, Benson A, Savani RC, Hooper LV, Yarovinsky F. Proteobacteria-specific IgA regulates maturation of the intestinal microbiota. Gut Microbes. 2014 Jan-Feb;5(1):28-39*
34. *Macpherson AJ, Hunziker L, McCoy K, Lamarre A. IgA responses in the intestinal mucosa against pathogenic and non-pathogenic microorganisms. Microbes Infect. 2001 Oct;3(12):1021-35*
35. *Cahenzli J, Balmer ML, McCoy KD. Microbial-immune cross-talk and regulation of the immune system. Immunology. 2013 Jan;138(1):12-22*

36. *Mowat AM, Agace WW. Regional specialization within the intestinal immune system. Nat Rev Immunol. 2014 Oct;14(10):667-85*
37. *Wells JM, Rossi O, Meijerink M, van Baarlen P. Epithelial crosstalk at the microbiota-mucosal interface. Proc Natl Acad Sci U S A. 2011 Mar 15;108 Suppl 1:4607-14*
38. *Cario E, Brown D, McKee M, Lynch-Devaney K, Gerken G, Podolsky DK. Commensal-associated molecular patterns induce selective toll-like receptor-trafficking from apical membrane to cytoplasmic compartments in polarized intestinal epithelium. Am J Pathol. 2002 Jan;160(1):165-73*
39. *Ozinsky A, Underhill DM, Fontenot JD, Hajjar AM, Smith KD, Wilson CB, Schroeder L, Aderem A. The repertoire for pattern recognition of pathogens by the innate immune system is defined by cooperation between toll-like receptors. Proc Natl Acad Sci U S A. 2000 Dec 5;97(25):13766-71*

40. *Feuillet V, Medjane S, Mondor I, Demaria O, Pagni PP, Galán JE, Flavell RA, Alexopoulou L. Involvement of Toll-like receptor 5 in the recognition of flagellated bacteria. Proc Natl Acad Sci U S A. 2006 Aug 15;103(33):12487-92*
41. *Rakoff-Nahoum, Paglino J, Eslami-Varzaneh F, Edberg S, Medzhitov R. Recognition of commensal microflora by toll-like receptors is required for intestinal homeostasis. Cell. 2004 Jul 23;118(2):229-41*
42. *Abreu MT, Arnold ET, Chow JY, Barrett KE. Phosphatidylinositol 3-kinase-dependent pathways oppose Fas-induced apoptosis and limit chloride secretion in human intestinal epithelial cells. Implications for inflammatory diarrheal states. J Biol Chem. 2001 Dec 14;276(50):47563-74*
43. *Melmed G Thomas LS, Lee N, Tesfay SY, Lukasek K, Michelsen KS, Zhou Y, Hu B, Arditi M, Abreu MT. Human intestinal epithelial cells are broadly unresponsive to Toll-like receptor 2-dependent bacterial ligands: implications for host-microbial interactions in the gut. J Immunol. 2003 Feb 1;170(3):1406-15.*
44. *Gewirtz AT, Navas TA, Lyons S, Godowski PJ, Madara JL. Cutting edge: bacterial flagellin activates basolaterally expressed TLR5 to induce epithelial proinflammatory gene expression. J Immunol. 2001 Aug 15;167(4):1882-*
45. *Artis D, Grencis RK. The intestinal epithelium: sensors to effectors in nematode infection. Mucosal Immunol. 2008 Jul;1(4):252-64*
46. *Neish AS, Gewirtz AT, Zeng H, Young AN, Hobert ME, Karmali V, Rao AS, Madara JL. Prokaryotic regulation of epithelial responses by inhibition of IkappaB-alpha ubiquitination. Science. 2000 Sep 1;289(5484):156*
47. *Zeuthen LH, Fink LN, Frøkiaer H. Toll-like receptor 2 and nucleotide-binding oligomerization domain-2 play divergent roles in the recognition of gut-derived lactobacilli and bifidobacteria in dendritic cells. Immunology. 2008 Aug;124(4):489-502*
48. *Furusawa Y, Obata Y, Fukuda S, Endo TA, Nakato G, Takahashi D, Nakanishi Y, Uetake C, Kato K, Kato T, Takahashi M, Fukuda NN, Murakami S, Miyauchi E, Hino S, Atarashi K, Onawa S, Fujimura Y, Lockett T, Clarke JM, Topping DL, Tomita M, Hori S, Ohara O, Morita T, Koseki H, Kikuchi J, Honda K, Hase K, Ohno H. Commensal microbe-derived butyrate*

induces the differentiation of colonic regulatory T cells. Nature. 2013 Dec 19;504(7480):446-50

49. *Macpherson AJ and Uhr T. Compartmentalization of the mucosal immune responses to commensal intestinal bacteria. Ann N Y Acad Sci. 2004 Dec;1029:36-43*
50. *Hooper LV and Macpherson AJ, Immune adaptations that maintain homeostasis with the intestinal microbiota. Nat Rev Immunol. 2010 Mar;10(3):159-69*
51. *Song Y, Shi YH, He C, Liu CQ, Wang JS, Zhao YJ, Guo YM, Wu RJ, Feng XY, Liu ZJ. Severe Henoch-Schönlein purpura with infliximab for ulcerative colitis. World J Gastroenterol. 2015 May 21;21(19):6082-7*
52. *Eisenhauer EA, Therasse P, Bogaerts J, et al. New response evaluation criteria in solid tumours: revised RECIST guideline (version 1.1). Eur J Cancer 2009; 45:228-47*